

# 1 **Green leaf area index estimation in maize and soybeans: combining vegetation** 2 **indices to achieve maximal sensitivity**

3 Anthony Nguy-Robertson, Anatoly Gitelson\*, Yi Peng, Andrés Viña, Timothy Arkebauer,  
4 Donald Rundquist

## 5 **Abstract**

6 Vegetation indices (VIs), traditionally used for estimation of green leaf area index (gLAI), have  
7 different sensitivities along the range of gLAI variability. The goals of this study were to: (1) test  
8 twelve VIs for estimating maize and soybean gLAI; (2) estimate gLAI in both crops without the  
9 need to re-parameterize the model for different crops; and (3) devise a combined VI that is  
10 maximally sensitive to gLAI along its entire range of variability. The study was performed for  
11 eight growing seasons (2001-2008) in one irrigated and one rainfed field under a maize/soybean  
12 rotation and one irrigated field under continuous maize in eastern Nebraska, USA, for a total of  
13 24 field-years. The gLAI ranged from 0 to 6.5 m<sup>2</sup>/m<sup>2</sup> in maize and 0 to 5.5 m<sup>2</sup>/m<sup>2</sup> in soybean.  
14 Normalized difference indices (e.g., NDVI) were most sensitive to gLAI below 2 m<sup>2</sup>/m<sup>2</sup> while  
15 ratio indices, e.g., Simple Ratio (SR) and Chlorophyll Indices (CI), were most sensitive to gLAI  
16 above 2 m<sup>2</sup>/m<sup>2</sup>. For the crops evaluated, relationships between gLAI and VIs were species-  
17 specific with the exception of the Red Edge NDVI and the CI<sub>red edge</sub>. In order to benefit from the  
18 different sensitivities of VIs along the entire gLAI range, we suggest combining VIs. For sensors  
19 with spectral bands in the red and NIR regions, the best combination was NDVI and SR (maize:  
20 coefficient of variation, CV = 20%; soybean: CV = 23%). However, this combined index is  
21 species-specific. For sensors with bands in the red edge and NIR regions, the best combination  
22 was Red Edge NDVI and CI<sub>red edge</sub>, which was capable of accurately estimating gLAI in both  
23 crops (i.e., maize and soybean) with a CV below 20% and with no re-parameterization.

24 Anthony Nguy-Robertson, Anatoly Gitelson, Yi Peng, and Donald Rundquist, Center for  
25 Advanced Land Management Information Technologies, School of Natural Resources,

26 University of Nebraska-Lincoln, Lincoln, Nebraska, 688588-0973, USA; Anthony Nguy-  
27 Robertson, Anatoly Gitelson, Yi Peng, and Donald Rundquist, School of Natural Resources,  
28 University of Nebraska-Lincoln, Lincoln, Nebraska, U.S.A; Andrés Viña, Center for Systems  
29 Integration and Sustainability, Department of Fisheries and Wildlife, Michigan State University,  
30 East Lansing, Michigan, U.S.A; Timothy Arkebauer, Department of Agronomy and Horticulture,  
31 University of Nebraska-Lincoln, Lincoln, Nebraska, U.S.A. Received \_\_\_\_\_. \*Corresponding  
32 author (agitelson2@unl.edu).

33

34 **Key words:** green leaf area index, vegetation indices, reflectance, MODIS, MERIS, noise  
35 equivalent.

36 **Abbreviations:** Leaf area index (LAI), green LAI (gLAI), vegetation index (VI), normalized  
37 difference vegetation index (NDVI), enhanced vegetation index 2 (EVI2), triangular vegetation  
38 index (TVI), modified TVI (MTVI), Chlorophyll Indices (CI), MERIS Terrestrial Chlorophyll  
39 Index (MTCI), Moderate Resolution Imaging Spectroradiometer (MODIS), Medium Resolution  
40 Imaging Spectroradiometer (MERIS), intensive measurement zones (IMZ), coefficients of  
41 determination ( $R^2$ ), standard error (SE), coefficient of variation (CV), noise equivalent (NE), root  
42 mean square error (RMSE), combined vegetation index (CVI), near infrared (NIR).

43

44 The leaf area index (LAI), the ratio of leaf area per ground area, typically reported with  
45 the units  $m^2/m^2$ , is a commonly used biophysical characteristic of vegetation (Watson, 1947).

46 LAI can be subdivided into photosynthetically active and photosynthetically inactive  
47 components. The former, termed green LAI (gLAI), is a metric commonly used in climate (e.g.  
48 Buermann et al., 2001), ecological (e.g. Bulcock and Jewitt, 2010), and crop yield (e.g. Fang et  
49 al., 2011) models. Because of its wide use and applicability to modeling, there is a need for a  
50 non-destructive remote estimation of gLAI over large geographic areas.

51 Various techniques based on remotely sensed data have been employed for assessing  
52 gLAI (see reviews in Pinter et al., 2003; Hatfield et al, 2004; 2008; Doraiswamy et al., 2003; Le  
53 Maire et al., 2008 and references within). Vegetation indices (VIs), particularly the normalized  
54 difference vegetation index, NDVI (Rouse et al., 1973) and the simple ratio, SR (Jordan, 1969)  
55 are the most widely used. However, NDVI is prone to saturation at moderate-to-high gLAI  
56 values (Kanemasu, 1974; Curran and Steven, 1983; Asrar et al., 1984; Huete et al., 2002;  
57 Gitelson, 2004; Wu et al., 2007; González-Sanpedro et al., 2008) and requires re-  
58 parameterization for different crops/species. The saturation of NDVI has been attributed to  
59 insensitivity of reflectance in the red region at moderate-to-high gLAI values due to the high  
60 absorption coefficient of chlorophyll. For gLAI below  $3 \text{ m}^2/\text{m}^2$ , total absorption by a canopy in  
61 the red range reaches 90-95% and further increases in gLAI do not bring additional changes in  
62 absorption and reflectance (Hatfield et al., 2008; Gitelson, 2011). Another reason for the  
63 decrease in sensitivity of NDVI to moderate-to-high gLAI values is the mathematical  
64 formulation of that index. At moderate-to-high gLAI, the NDVI is dominated by near infrared  
65 (NIR) reflectance. Because scattering by cellular/leaf structure causes the NIR reflectance to be  
66 high and the absorption by chlorophyll causes the red reflectance to be low, NIR reflectance is  
67 considerably greater than red reflectance: e.g., for  $\text{gLAI} = 3 \text{ m}^2/\text{m}^2$ , NIR reflectance is around  
68 40%, while red reflectance is below 5%. Thus, NDVI becomes insensitive to changes in both red  
69 and NIR reflectances.

70 Other commonly used VIs include the enhanced vegetation index, EVI (Huete et al.,  
71 1997; 2002), its alternative form, EVI2 (Jiang et al., 2008), and the triangular vegetation index,  
72 TVI (Broge and Leblanc, 2001). While the EVI is more sensitive to moderate-to-high LAI than  
73 NDVI, it was also found to be sensitive to canopy architecture (Gao et al., 2000), and it does not

74 relate well to LAI during the senescence stages (Wang et al., 2005). The TVI relates the  
75 difference between reflectance in the NIR and red regions to the magnitude of reflectance in the  
76 green region, thus, defining a triangle in a three dimensional spectral space. While the TVI is less  
77 affected by atmospheric properties when compared to typical vegetation indices, it is sensitive to  
78 differences in canopy structure and soil background (Broge and Leblanc, 2001). To minimize the  
79 sensitivities of TVI, a soil adjustment factor has been introduced in a modified version of the  
80 TVI, MTVI (Haboudane et al., 2004). The same study found that a second modified version  
81 (MTVI2) was accurate in estimating gLAI in different canopy structures that were simulated  
82 through radiative transfer models. Another investigation, aimed at examining gLAI in wheat,  
83 found that MTVI2 was more sensitive than NDVI to gLAI at higher gLAI values; however, it  
84 was sensitive to heading (i.e. flowering), which is not a component of gLAI, but nevertheless  
85 affects the reflectance of crop canopies (Smith et al., 2008).

86 VIs that incorporate bands in the spectral transition zone between absorption by pigments  
87 and scattering by leaves/canopies, termed the “red edge region” (between 700 and 740 nm), were  
88 introduced to increase the sensitivity to moderate-to high vegetation densities and estimate total  
89 chlorophyll content and gLAI (Gitelson and Merzlyak, 1994; Gitelson et al., 2003; Dash and  
90 Curran, 2004). Radiation in the red edge region penetrates deeper into the leaves and canopies  
91 than radiation in the visible region due to a lower absorption coefficient in the former than in the  
92 latter. Thus, higher values of chlorophyll content and gLAI are required to decrease the  
93 sensitivity of red edge VIs to gLAI (Dash and Curran, 2004; Ciganda et al., 2008; Gitelson,  
94 2011). Some of the red edge VIs constitute transformations of existing VIs, such as the red edge  
95 NDVI (Gitelson and Merzlyak, 1994), which replaces the red band with one in the red edge  
96 region. Others constitute semi-analytical procedures for estimating pigment content in diffuse

97 media, such as the Chlorophyll Indices, CI (Gitelson et al., 2003a). While the CIs were  
98 developed for estimating chlorophyll content, they also relate closely with gLAI since total  
99 canopy chlorophyll content has been shown to relate closely with the gLAI (Ciganda et al., 2008;  
100 Peng et al., 2011). Therefore, CIs are suitable for estimating gLAI (Gitelson et al., 2003b;  
101 Brantley et al., 2011), but particularly for moderate-to-high gLAI values. For instance, it was  
102 found that VIs utilizing the red edge region (710-730 nm) were more accurate for estimating  
103 moderate-to-high gLAI in shrub canopies than normalized difference indices (Brantley et al.,  
104 2011). However, this study also found that at low-to-moderate gLAI values, normalized  
105 difference indices (e.g., NDVI) perform better than the  $CI_{red\ edge}$ . The MERIS Terrestrial  
106 Chlorophyll Index (MTCI) also contains a red-edge band, and was developed for the remote  
107 estimation of total canopy chlorophyll content (Dash and Curran, 2004; 2007). It has been shown  
108 that the MTCI closely relates with gLAI (Gitelson, 2011).

109 For gLAI estimation using VIs, it is ideal that the VI selected is not sensitive to canopy  
110 architecture (e.g. leaf angle distribution), leaf structure (e.g. foliar chlorophyll distribution), and  
111 heliotropism (e.g. sun-avoidance), so that the relationships gLAI vs. VI would be applicable to  
112 different vegetation types without requiring algorithm re-parameterization. The VIs selected  
113 should also be insensitive to soil background and atmospheric effects.

114 To minimize the effects of soil background and maximize the sensitivity to foliar  
115 chlorophyll, Daughtry et al. (2000) suggested combining two VIs by taking a ratio of a VI  
116 sensitive to chlorophyll and a VI insensitive to soil background, canopy architecture, and LAI  
117 variability. Thus, combination of indices based on the Transformed Chlorophyll Absorption  
118 Reflectance Index (TCARI), the MCARI, and the OSAVI, such as, TCARI/OSAVI and  
119 MCARI/OSAVI, were used to estimate leaf chlorophyll content in crops, minimizing the effects

120 of the soil background and the green LAI variation (Daughtry et al., 2000; Haboudane et al.,  
121 2002). However, the goal of these studies was to remove the effect of LAI on the estimation of  
122 leaf chlorophyll content (Daughtry et al., 2000; Haboudane et al., 2002; Eitel et al., 2008; 2009),  
123 therefore, for this study, that particular set of VIs was not considered for estimating gLAI.

124 Viña et al., (2011) evaluated the potential effects of soil background on the remote  
125 estimation of gLAI. For this, they used reflectance spectra of spherical and planophile canopies  
126 with different gLAI values under two contrasting soil backgrounds (i.e., dark and bright), as  
127 simulated by the New Advanced Discrete Model (Gobron et al. 1997), and used them for  
128 calculating three vegetation indices - EVI, MTCI and  $CI_{red\ edge}$ . The EVI has been suggested to  
129 be less sensitive to background effects (Huete et al. 1997), however, the uncertainties of gLAI  
130 estimation due to soil background effects by all three indices were very similar. In the spherical  
131 canopy, the errors of EVI, MTCI and  $CI_{red\ edge}$  were 0.25, 0.18, and  $0.21\ m^2/m^2$ , respectively,  
132 while in the planophile canopy they were 0.21, 0.20,  $0.14\ m^2/m^2$ , respectively.

133 Maize and soybean plants have contrasting canopy architectures (i.e., maize has a  
134 predominantly spherical leaf angle distribution while soybean has a predominantly  
135 planophile/heliotropic leaf angle distribution), and leaf structures (i.e., maize is a monocot while  
136 soybean is a dicot) that exhibit different chlorophyll distributions along the leaf depth (de Wit,  
137 1965; Idso and de Wit, 1970; Ehleringer and Forseth, 1980). Additionally, these two species  
138 have different physiological pathways (C3 vs. C4). Based on contrasting anatomical and  
139 physiological traits, these crops are representative of many crops types, and most VIs have been  
140 shown to respond to them, thus are species- or crop-specific (Curran and Milton, 1983; Gao et  
141 al., 2000; González-Sanpedro et al., 2008). However, some indices that use red edge bands in

142 their formulation have been shown to be less sensitive to differences among species (Gitelson et  
143 al., 2005; Gitelson, 2011; Brantley et al., 2011; Viña et al., 2011).

144 The objectives of this study were to: (1) test the performance of twelve VIs for estimating  
145 gLAI in maize (*Zea mays*) and soybean (*Glycine max*); (2) identify an algorithm that does not  
146 require re-parameterization for estimating gLAI in both maize and soybean (C3 vs C4 crops);  
147 and (3) devise a “combined vegetation index” that is maximally sensitive to gLAI along its entire  
148 range of variability (i.e. 0 to more than 6 m<sup>2</sup>/m<sup>2</sup>), and is applicable to current operational  
149 satellite-based sensors such as the Moderate Resolution Imaging Spectroradiometer (MODIS) on  
150 board the National Aeronautics and Space Administration (NASA) Terra and Aqua satellites, or  
151 the European Space Agency (ESA) Medium Resolution Imaging Spectroradiometer (MERIS).

152

## 153 **Materials and Methods**

154 The study area is located at the University of Nebraska-Lincoln (UNL) Agricultural  
155 Research and Development Center near Mead, Nebraska, U.S.A. It consists of three 65-ha fields  
156 under different management practices (Table 1). The soils are deep silty clay loams including  
157 Tomek, Yutan, Filbert, and Fillmore soil series (Suyker et al., 2004). During the years of study,  
158 field 1 was under continuous irrigated maize while fields 2 and 3 were under a maize/soybean  
159 rotation, with maize during odd years and soybean during even years. Field 2 was irrigated,  
160 while field 3 received only rainfall. Overall, there were nine maize hybrids and three soybean  
161 hybrids under different planting densities (Table 1). All crops were fertilized and treated with  
162 herbicide/pesticides following UNL’s best management practices for eastern Nebraska.

163 It has been reported that 2003 and 2005 were especially dry years, with annual  
164 precipitation values of 650 and 607 mm, respectively, which were well below the 1026 mm of a

165 “normal” year (Suyker and Verma, 2010). Thus, water stress occurred under low soil moisture  
166 conditions, which severely affected grain yield. For example, during dry periods in 2003, soil  
167 moisture at the 10 cm depth in the rainfed field dropped more than 40% compared to that in  
168 irrigated fields. The difference in daily gross primary production (GPP) between irrigated and  
169 rainfed fields increased during the dry periods and reached a peak value, which corresponded to  
170 40% of the maximal daily GPP value (Suyker and Verma, 2010). As a result, the ratio of grain  
171 yield in the irrigated field to that in the rainfed field was above 1.8 in 2003, while in a “normal”  
172 year with higher precipitation (e.g., 2007), it was below 1.3 (Suyker and Verma, 2010).

173 Six small (20 x 20 m) plots (henceforth referred to as intensive measurement zones,  
174 IMZs) were established in each field for performing detailed plant measurements. The IMZs  
175 represented all major soil and crop production zones within each field (Verma et al., 2005). The  
176 IMZ results were aggregated to a field mean based on a weighted average of the relative area of  
177 the stratified zones represented by each IMZ. The gLAI was calculated from sampling a 1 m  
178 length of one or two rows ( $6 \pm 2$  plants), located within each IMZ, every 10-14 days starting at  
179 the initial growth stages (V1-V3), based on the scale by Abendroth et al., (2011), and ending at  
180 crop maturity (R5-R7) in both species. Collection rows were alternated between sampling dates  
181 to minimize edge effects. The plants collected were transported on ice (to reduce pheophytin  
182 formation) to the laboratory where they were visually divided into green leaves, dead leaves,  
183 stems, and reproductive organs. The leaf area was measured using an area meter (Model LI-  
184 3100, LI-COR, Inc., Lincoln, NE), which was subsequently used to determine gLAI (green leaf  
185 area in  $\text{m}^2$  divided by ground area in  $\text{m}^2$ ) by multiplying the green leaf area per plant by the plant  
186 population (number of plants per  $\text{m}^2$ ) as counted in each IMZ (i.e. not based on planting density  
187 shown in Table 1). The values calculated from all six IMZs were averaged for each sampling



188 date to provide a field-level gLAI. During the eight years of the study, the mean standard error  
189 of gLAI measurements was less than  $0.15 \text{ m}^2/\text{m}^2$  (Guindin-Garcia et al., 2012). Cubic spline  
190 interpolation (in MATLAB<sup>®</sup>) was used to estimate values of gLAI corresponding to days of  
191 reflectance measurement when that parameter was not acquired concurrently with the destructive  
192 gLAI determination.

193 Canopy reflectance was collected using an all-terrain sensor platform, equipped with a  
194 dual-fiber system and two Ocean Optics USB2000 spectroradiometers, with a spectral range of  
195 400-1100 nm and a spectral resolution of 1.5 nm (Rundquist et al., 2004). One fiber was fitted  
196 with a cosine diffuser to measure incoming downwelling irradiance, while the second one  
197 measured upwelling radiance. The field of view of the downward-pointing sensor was kept  
198 constant along the growing season (approximately 2.4 m in diameter) by placing the  
199 spectroradiometer at a height of 5.5 m above the top of the canopy. Radiometric data were  
200 collected close to solar noon (between 11:00 and 13:00 local time), when changes in solar zenith  
201 angle were minimal. Ten reflectance spectra were measured at each collection point along access  
202 roads into each of the fields, and computed average reflectance represented each collection point.  
203 Six randomly selected plots were established per field, each with six randomly selected sampling  
204 points. Thus, a total of 36 points within these areas were sampled per field at each data  
205 acquisition, and their median per date was used as the overall field reflectance. Measurements  
206 took about 5 minutes per plot and about 30 minutes per field. The two radiometers were inter-  
207 calibrated immediately before and immediately after measurement in each field. Reflectance  
208 measurements were carried out during the growing season each year over the eight-year period.  
209 This resulted in a total of 314 reflectance spectra for maize (47 in 2001, 30 in 2002, 92 in 2003,  
210 30 in 2004, 53 in 2005, 13 in 2006, 40 in 2007 and 9 in 2008) and 145 spectra for soybean (54 in

211 2002, 49 in 2004, 26 in 2006 and 16 in 2008), which were representative of a wide range of  
212 gLAI variation found in maize and soybean cropping systems.

213 Using hyperspectral aerial imagery, acquired over the study site by an AISA Eagle  
214 hyperspectral imaging spectrometer, it was shown that the canopy reflectance in the fields were  
215 spatially homogeneous; thus, reflectance spectra taken along access roads were representative of  
216 the field (Viña et al., 2011). Therefore, the remotely estimated gLAI may be compared with  
217 measured field level gLAI.

218 The twelve VIs examined in this study (Table 2) were chosen as they are representative  
219 of VIs that are widely used (e.g., NDVI, SR), some of them minimize soil background effects  
220 (e.g., OSAVI, EVI). They were also selected because of their applicability to data collected by  
221 satellite sensors such as MODIS and MERIS. These two sensors are utilized much more  
222 frequently than hyperspectral sensors, which are expensive to operate and cover limited study  
223 areas. Since a goal of this study was to find VIs applicable to MODIS and MERIS, the collected  
224 field reflectance spectra were resampled by averaging the Ocean Optics data to simulate the  
225 spectral bands of MODIS (band 3/green: 545 - 565 nm, band 1/red: 620 - 670 nm, and band  
226 2/NIR: 841 - 876 nm) and of MERIS (band 5/green: 555 - 565 nm, band 7/red: 660 - 670 nm,  
227 band 8/red: 677.5-685, band 9/red edge: 703.8 - 713.8 nm, band 10 NIR: 750 - 757.5 nm, and  
228 band 12/NIR: 771.3 - 786.3).

229 Best-fit relationships between VIs and gLAI were determined using Eureqa (Schmidt and  
230 Lipson, 2009; <http://creativemachines.cornell.edu/eureqa>), an algorithm search engine that  
231 identifies and ranks potential regression models that best correspond to the input data. Users  
232 input the desired relationship, e.g.  $VI = f(gLAI)$ , along with potential operations (e.g. addition,  
233 subtraction, exponential, power, etc.) and an error metric (e.g. minimize absolute error,  $R^2$ , etc.).

234 In our case, the fitness metric used to rank the best-fit functions constituted the minimization of  
235 the root mean square error (RMSE). The inverse of these relationships (i.e., gLAI vs. VI) was  
236 utilized for gLAI estimation using VIs. After determining the best-fit relationships, a  $k$ -fold ( $k =$   
237 10) cross-validation procedure (Kohavi, 1995) was utilized to determine the estimates of model  
238 coefficients, coefficients of determination ( $R^2$ ), standard error (SE), and coefficients of variation  
239 (CV) using the statistical package R (V. 2.12.2, R Development Core Team 2011). CV is the  
240 standard deviation of the gLAI vs. VI relationship divided by mean value of gLAI. The data or  
241 subgroups (i.e., different crops - maize or soybean) were randomly divided into ten sets using a  
242 random sequence generator (random.org), nine of which were used iteratively for calibration and  
243 the remaining set for validation.

244 It is important to note that the  $R^2$  values, as well as SE and CV of gLAI estimation,  
245 represent the dispersion of the points from the best-fit regression lines. They constitute measures  
246 of how good the regression model (best-fit function) is in capturing the relationship between  
247 gLAI and VI. However, when the best-fit function is nonlinear, the  $R^2$  as well as the SE values  
248 may be misleading. To determine the accuracy of gLAI estimation, we employed the noise  
249 equivalent (NE) of gLAI (Govaerts et al., 1999; Viña and Gitelson, 2005), that was calculated as:  
250 
$$NE \Delta gLAI = RMSE(VI \text{ vs. } gLAI) / [d(VI)/d(LAI)] \quad (1)$$

251 Where  $d(VI)/d(gLAI)$  is the first derivative of VI with respect to gLAI and  $RMSE(VI \text{ vs. } LAI)$  is  
252 the root mean square error of the VI vs gLAI relationship. The  $NE \Delta gLAI$  provides a measure of  
253 how well the VI responds to gLAI across its entire range of variation.  $NE \Delta gLAI$  takes into  
254 account not only the RMSE of gLAI estimation but also accounts for the sensitivity of the VI to  
255 gLAI, thus providing a metric accounting for both scattering of the points from the best fit  
256 function and the slope of the best fit function.

257 To test the applicability of VIs to estimate the gLAI of different crops with no algorithm  
258 re-parameterization, we performed an analysis of variance (ANOVA) between the coefficients of  
259 the best-fit function for both species (maize and soybean) combined, versus the coefficients  
260 obtained for each individual crop (Ritz and Streibig, 2008).

261

## 262 **Results and Discussion**

263 While both maize and soybean undergo three major stages of development (green-up,  
264 reproductive, and senescence), the temporal dynamics of their gLAI are very different (Fig. 1). In  
265 maize, the green-up period was longer (~20 days) than in soybean. Maize remained in the  
266 vegetative stage as gLAI increased until it reached the maximum gLAI, which occurred when  
267 silking began. There was a decrease in gLAI of about  $1 \text{ m}^2/\text{m}^2$  during the kernel development.  
268 Then, during the final stage before maturity (dent), gLAI dropped to nearly  $0 \text{ m}^2/\text{m}^2$  (Fig. 1a). In  
269 contrast, soybean flowered before maximum gLAI was reached, which occurred during pod and  
270 seed development, and decreased once the plant reached full seed (Fig. 1b). The ranges of maize  
271 and soybean gLAI variability were also different. In irrigated maize, the maximum gLAI reached  
272  $6.5 \text{ m}^2/\text{m}^2$  while in soybean it did not exceed  $5.5 \text{ m}^2/\text{m}^2$ . For both crops, gLAI maxima in rainfed  
273 fields were typically lower than in irrigated fields (Fig. 1, Table 1). Thus, the maximum gLAI  
274 differed on per crop (i.e., maize vs. soybean) and water status (i.e. irrigated vs. rainfed) bases.

275 All best-fit functions established between gLAI and VI for either maize (Table 3) or  
276 soybean (Table 4) were non-linear, and the shapes of the relationships VI vs gLAI differed  
277 among VIs (Fig. 2). For example, NDVI reached an asymptote at around 0.7 when gLAI was  
278 between  $2$  and  $3 \text{ m}^2/\text{m}^2$ , and became almost invariant for  $\text{gLAI} > 4 \text{ m}^2/\text{m}^2$  in both maize and  
279 soybean (Fig. 2b). This saturation of the NDVI (Fig. 2b) reduces its functionality for gLAI

280 estimation at moderate-to-high gLAI values, since it generates large uncertainty in model  
281 inversions: almost the same value of VI corresponds to gLAI ranging from 4 to more than 6  
282  $\text{m}^2/\text{m}^2$ . Several other normalized difference indices (green NDVI, red edge NDVI, EVI2, and  
283 WDRVI with  $\alpha = 0.2$ ), TVI and MTVI2 also showed different degrees of decreased sensitivity at  
284 moderate-to-high gLAI values (Figs 2c, d, e, h, j, k, l). SR had an exponential relationship with  
285 lower sensitivity to  $\text{gLAI} < 1 \text{ m}^2/\text{m}^2$  than to higher gLAI values (Fig. 2a). For  $\text{gLAI} > 1 \text{ m}^2/\text{m}^2$ ,  
286 the relationship between SR and gLAI was nearly linear. The relationships for CIs and the MTCI  
287 exhibited a similar shape, with an increase in slope at moderate to high gLAI (Figs. 2f, g, i).

288 In this study, we found that among the twelve VIs examined, only the red edge NDVI  
289 (ANOVA:  $p = 0.36$ ,  $n = 423$ ,  $F = 1.09$ ) and the  $\text{CI}_{\text{red edge}}$  (ANOVA:  $p = 0.11$ ,  $n = 423$ ,  $F = 1.65$ )  
290 can be applied for maize and soybean with no re-parameterization of the model. Best-fit  
291 functions of the relationships gLAI vs. red Edge NDVI and  $\text{CI}_{\text{red edge}}$  for both maize and soybean  
292 are presented in Table 5. All other VIs were crop-specific (ANOVA:  $p < 0.001$ ,  $n = 423$ ,  $F >$   
293 4.5).

294 As noted in the Materials and Methods section,  $R^2$  and SE may be misleading when  
295 comparing non-linear and linear relationships. For example, although the relationship NDVI vs  
296 gLAI resulted in high  $R^2$  values, the slope of the relationship decreased as gLAI exceeded 3  
297  $\text{m}^2/\text{m}^2$  and became close to zero at gLAI values above 3.5  $\text{m}^2/\text{m}^2$  for soybean and above 4  $\text{m}^2/\text{m}^2$   
298 for maize (Fig. 2b). With the decrease in sensitivity of VIs to gLAI (i.e., when gLAI exceeds 3  
299  $\text{m}^2/\text{m}^2$ ), the scattering of the points from the best-fit functions drops, as can be seen for NDVI,  
300 green NDVI, red edge NDVI and OSAVI (Figs. 2b, 2c, 2d, and 2e, for soybean). Thus, most of  
301 the VIs had similar  $R^2$  and SE (Tables 3 and 4) but very different shapes of the relationships VI  
302 vs gLAI (e.g., increasing exponential decay in NDVI vs. exponential growth in SR). Therefore, a

303 different accuracy metric, specifically the NE  $\Delta$ gLAI, was needed to compare the performance of  
304 VIs in estimating gLAI along its entire range of variation.

305 Fig. 3 displays values of NE  $\Delta$ gLAI for normalized difference VIs, MTCI and ratio  
306 indices (SR, CIs). TVI and MTVI2 were not included in this analysis because their NE  $\Delta$ gLAI  
307 values were always greater than those of normalized difference indices at low to moderate gLAI,  
308 and also were always greater than those of SR, CIs and MTCI at moderate to high gLAI.  
309 Therefore, TVI and MTVI2 did not meet the criteria for determining the best indices either for  
310 low-to-moderate, for moderate-to-high, or for the entire range of gLAI.

311 The normalized difference VIs had asymptotic relationships with gLAI (Figs. 2b, c, d, h,  
312 l); thus, the NE  $\Delta$ gLAI was lowest at gLAI below  $2.5 \text{ m}^2/\text{m}^2$  for maize and below  $2 \text{ m}^2/\text{m}^2$  for  
313 soybean (Fig. 3). SR and CIs had exponential relationships with gLAI (Figs. 2a, f, g); thus, the  
314 lowest values of NE  $\Delta$ gLAI were at gLAI exceeding  $3 \text{ m}^2/\text{m}^2$  (Fig. 3). Therefore, the normalized  
315 difference VIs were more accurate in estimating low-to-moderate gLAI while the ratio indices,  
316 SR and CIs, were more accurate in estimating moderate-to-high gLAI.

317 While the relationship of MTCI with gLAI was asymptotic, the slope of the relationship  
318 was almost constant in a wide range of gLAI variation (Fig. 2i). Therefore, for MTCI, NE  $\Delta$ gLAI  
319 varied little throughout the entire range of gLAI (Fig. 3). In the range of gLAI below  $2.5 \text{ m}^2/\text{m}^2$ ,  
320 the MTCI had lower accuracy than normalized difference VIs and almost the same accuracy as  
321 SR and CI indices. However, in the range of gLAI  $> 2.5 \text{ m}^2/\text{m}^2$ , it had lower accuracy than SR  
322 and CIs. Thus, it did not outperform normalized difference VIs or SR and CI indices in their  
323 respective regions of highest sensitivity to changes in gLAI.

324 At moderate to high gLAI, the noise equivalents of normalized difference indices in  
325 soybean were higher than those in maize. This may be explained by the very different canopy

326 architectures and leaf structures of these crops. For the same amount of foliar chlorophyll  
327 content, the chlorophyll density on the adaxial side of soybean leaves is higher than that in maize  
328 leaves, causing a higher absorption in the red range and thus lower reflectance of soybean  
329 canopies: 2% for leaf chlorophyll above  $500 \text{ mg/m}^2$  (Gitelson et al., 2005) compared to 3-5% of  
330 maize leaves. In addition, for the same gLAI, canopy reflectance of soybean in the NIR region  
331 was higher than that of maize: for gLAI around  $5 \text{ m}^2/\text{m}^2$ , NIR reflectance was 60% in soybean  
332 vs. 40% in maize (Peng and Gitelson, 2011). Thus, for the same gLAI, especially within the  
333 moderate-to-high range, a NIR to red reflectance ratio is higher in soybean than in maize.  
334 Therefore, the value of gLAI above which the normalized difference indices became insensitive  
335 to gLAI was lower in soybean than in maize.

336 Analysis of the NE  $\Delta\text{gLAI}$  of VIs (Fig. 3) showed that for gLAI below  $2.5 \text{ m}^2/\text{m}^2$ ,  
337 normalized difference VIs had the lowest NE  $\Delta\text{gLAI}$ , and thus highest accuracy of gLAI  
338 estimation, while SR and CIs had the highest accuracy for gLAI  $> 3 \text{ m}^2/\text{m}^2$  and were the best  
339 suited for estimation of moderate-to-high gLAI. Therefore, there was no single index that had the  
340 lowest uncertainties of gLAI estimation along the entire range of gLAI variation. In order to  
341 obtain the highest possible accuracy (i.e., lowest NE  $\Delta\text{gLAI}$ ) across the entire range of gLAI, we  
342 suggest using more than one VI in combination, i.e., a combined vegetation index (CVI).

343 The CVI is comprised of two VIs that are the most accurate in gLAI estimation at  
344 different ranges of gLAI: the first index for low-to-moderate gLAI (below  $2.5 \text{ m}^2/\text{m}^2$ ) and the  
345 second index for moderate-to-high gLAI (above  $2.5 \text{ m}^2/\text{m}^2$ ). While it is possible to scale the VIs  
346 in CVI to create a linear relationship, any scaled algorithm will be data-set dependent and may  
347 result in a decrease in the sensitivity of the VI to gLAI. For both MODIS and MERIS data,  
348 containing the red and NIR bands, we suggest using NDVI as the first index and SR as the

349 second index - CVI{NDVI, SR}. An NDVI value around 0.7 has been previously reported as a  
350 typical point where the NDVI vs. green LAI relationship becomes saturated (Myneni et al., 1995;  
351 Gitelson et al., 2003b). Therefore, we selected NDVI = 0.7 as a threshold for both maize and  
352 soybeans. In the range of NDVI from 0 to 0.7, the best fit functions of NDVI vs. gLAI for both  
353 crops were linear and, thus, NE  $\Delta$ gLAI was constant and as low as  $0.38 \text{ m}^2/\text{m}^2$  for maize (Fig.  
354 4a) and  $0.4 \text{ m}^2/\text{m}^2$  for soybean (Fig. 4b).

355 As gLAI exceeded  $2.5 \text{ m}^2/\text{m}^2$ , the NE  $\Delta$ gLAI of SR decreased and the accuracy of gLAI  
356 estimation increased for both species (Figs. 4a and b). When SR was above 5.7 (corresponding to  
357 NDVI = 0.7), the best-fit function of SR vs. gLAI was linear and, thus, NE  $\Delta$ gLAI was constant  
358 and equal to  $0.68 \text{ m}^2/\text{m}^2$  for maize (Fig. 4a) and  $0.49 \text{ m}^2/\text{m}^2$  for soybean (Fig. 4b). A CVI  
359 comprised of two indices (NDVI and SR and, thus, using only red and NIR bands), was able to  
360 estimate gLAI ranging from 0 to more than  $6 \text{ m}^2/\text{m}^2$  with a RMSE below  $0.72 \text{ m}^2/\text{m}^2$  and a CV  
361 of 20% for maize, and a RMSE below  $0.54 \text{ m}^2/\text{m}^2$  and a CV of 23% for soybean. However, the  
362 algorithms relating gLAI and CVI{NDVI, SR} for maize and soybean required different  
363 coefficients (Table 6) and, thus, were crop specific.

364 Alternatively, we suggest using the red edge NDVI as the first CVI index and the  $CI_{\text{red}}$   
365 <sub>edge</sub> as the second CVI index – i.e., CVI{red edge NDVI,  $CI_{\text{red}}$  <sub>edge</sub>} (Fig. 5) for data acquired by  
366 sensor systems containing red edge and NIR bands (e.g., MERIS, HYPERION). This combined  
367 index was not crop-specific at least for the species evaluated (i.e., maize and soybean), which  
368 have quite contrasting leaf and canopy structures. Therefore, this CVI does not require re-  
369 parameterization, since the same algorithm coefficients can be applied to estimate gLAI in both  
370 crops (Table 6). Based on the NE  $\Delta$ gLAI results, presented in Fig. 5, we suggest using a  
371 threshold of red edge NDVI equal to 0.6. For the range of red edge NDVI of 0 to 0.6, the NE



372  $\Delta$ gLAI was  $0.46 \text{ m}^2/\text{m}^2$  and for  $CI_{\text{red edge}}$  above 3 (corresponding to the red edge NDVI value of  
373 0.6) the NE  $\Delta$ gLAI was  $0.55 \text{ m}^2/\text{m}^2$  (Fig. 5). For both species,  $CVI\{\text{red edge NDVI}, CI_{\text{red edge}}\}$   
374 was able to estimate gLAI along its entire range of variation (i.e., 0 to  $> 6 \text{ m}^2/\text{m}^2$ ), with a RMSE  
375 below  $0.60 \text{ m}^2/\text{m}^2$  and a CV of 19%.

376 In applications where prior knowledge about crop type is available, using sensor systems  
377 containing red and NIR bands with spatial resolutions high enough to reduce the effects of mixed  
378 pixels, the  $CVI\{\text{NDVI}, SR\}$  is adequate. However, in many cases, there is uncertainty about the  
379 crop type present within a pixel (e.g., coarse spatial resolutions, mixed pixels, areas of crop  
380 rotation without prior knowledge of planted crops). Thus, the  $CVI\{\text{red edge NDVI}, CI_{\text{red edge}}\}$ ,  
381 having a unified algorithm for crops with different leaf and canopy structures (e.g., maize and  
382 soybean), brings an objective estimation of total gLAI, even in the case of mixed pixels and  
383 crops at different phenological stages.

384 We acknowledge that further research is needed to evaluate the  $CVI\{\text{red edge NDVI},$   
385  $CI_{\text{red edge}}\}$  in other crops. However, since in this study it was tested in crops that are very  
386 different (maize and soybean), it will likely be insensitive to leaf and canopy structure of crops  
387 that are not as different. It is also important to investigate the reliability of the CVIs developed  
388 when applied to estimating gLAI in other vegetation types, such as grasslands and forests.  
389 Additionally, the calibration equations for the CVIs built with simulated MODIS and MERIS  
390 bands obtained from close-range hyperspectral data should be tested against actual MODIS and  
391 MERIS data. However, it is likely that these equations are reliable since it has been shown that  
392 the coefficients of the relationships between gLAI and WDRVI, when taken at close range,  
393 remained the same as those applied to MODIS 250 m data, due to accurate atmospheric

394 correction of the MODIS 250 m surface reflectance product (Gitelson et al., 2007; Guindin-  
395 Garcia et al., 2012).

396 The approach presented in this study is not limited to gLAI, as it may also be used for the  
397 remote estimation of other biophysical characteristics, such as vegetation cover, fraction of  
398 absorbed photosynthetically active radiation and gross primary production. Nevertheless, the  
399 CVIs presented in this study may not constitute the best vegetation index combinations for  
400 measuring these other vegetation characteristics. Therefore, future studies are needed to  
401 investigate which VI combinations are the most appropriate for assessing other biophysical  
402 characteristics of vegetation.

403

## 404 **Conclusions**

405 Twelve vegetation indices, calculated from simulated spectral bands of MODIS and  
406 MERIS satellite sensor systems, were evaluated for remotely assessing gLAI in two crop species  
407 with contrasting leaf structures and canopy architectures. All VIs investigated had essentially  
408 non-linear relationships with gLAI, although with different sensitivities along the range of gLAI  
409 variability evaluated. On this basis, we suggest combining vegetation that exhibit high sensitivity  
410 to changes in green LAI at particular ranges (i.e., low-to-moderate and moderate-to-high). When  
411 combined, these indices constitute suitable and accurate remotely sensed surrogates of gLAI  
412 along its entire range of variability. Specifically we suggest combining the NDVI and the SR,  
413  $\text{CVI}\{\text{NDVI}, \text{SR}\}$  to be used in the case of sensors with spectral bands in the red and NIR (e.g.,  
414 MODIS 250 m, Landsat TM and ETM+), although this combined index is crop-specific and  
415 requires re-parameterization of the algorithm for each crop. Alternatively, if a band in the red-  
416 edge region is available (e.g., MERIS, HYPERION), we suggest combining the red edge NDVI

417 and the  $CI_{\text{red edge}}$ ,  $CVI_{\text{red edge NDVI}}$ ,  $CI_{\text{red edge}}$ . Since it was not crop-specific, this combined  
418 index was capable of estimating gLAI with high accuracy, thus providing a suitable procedure  
419 for remotely estimating gLAI of crops with contrasting canopy architectures and leaf structures.

#### 420 **Acknowledgments**

421 This study was supported by NASA NACP grant No. NNX08AI75G and partially by the U.S.  
422 Department of Energy: (a) EPSCoR program, Grant No. DE-FG-02-00ER45827 and (b) Office  
423 of Science (BER), Grant No. DE-FG03-00ER62996. We acknowledge the support and the use of  
424 facilities and equipment provided by the Center for Advanced Land Management Information  
425 Technologies (CALMIT), and Carbon Sequestration Program, University of Nebraska-Lincoln.  
426 This research was also supported in part by funds provided through the Hatch Act. The Nebraska  
427 Space Grant has provided travel assistance for presenting these results. We are also thankful for  
428 the multitude of staff, graduate and undergraduate students involved in collecting the data used  
429 in the study.

430 **References**

- 431 Abendroth, L.J., R.W. Elmore, M.J. Boyeer, and S.K. Marlay. 2011. Corn growth and  
432 development. Publ. PMR 1009. Iowa State Univ. Ext., Ames.
- 433 Asrar, G.F., M. Kanemasu, and J. ET Hatfield. 1984. Estimating absorbed photosynthetic  
434 radiation and leaf area index from spectral reflectance in wheat. *Agron. J.* 76(2): 300-306.  
435 doi: 10.2134/agronj1984.00021962007600020029x
- 436 Brantley, S.T., J.C. Zinnert, and D.R. Young. 2011. Application of hyperspectral vegetation  
437 indices to detect variations in high leaf area index temperate shrub thicket canopies. *Remote*  
438 *Sens. Environ.* 115(2): 514-523. doi: 10.1016/j.rse.2010.09.020
- 439 Broge, N.H., and E. Leblanc. 2001. Comparing prediction power and stability of broadband and  
440 hyperspectral vegetation indices for estimation of green leaf area index and canopy  
441 chlorophyll density. *Remote Sens. Environ.* 76(2000): 156-172. doi: 10.1016/S0034-  
442 4257(00)00197-8
- 443 Buermann, W., J. Dong, X. Zeng, R.B. Myneni, and R.E. Dickinson. 2001. Evaluation of the  
444 Utility of Satellite-Based Vegetation Leaf Area Index Data for Climate Simulations. *J.*  
445 *Climate* 14(17): 3536-3550. doi: 10.1175/1520-0442(2001)014<3536:EOTUOS>2.0.CO;2
- 446 Bulcock, H.H., and G.P.W. Jewitt. 2010. Spatial mapping of leaf area index using hyperspectral  
447 remote sensing for hydrological applications with a particular focus on canopy interception.  
448 *Hydrol. Earth Syst. Sc.* 14(2): 383-392. doi:10.5194/hess-14-383-2010
- 449 Ciganda, V., A.A. Gitelson, and J. Schepers. 2008. Vertical Profile and Temporal Variation of  
450 Chlorophyll in Maize Canopy: Quantitative “Crop Vigor” Indicator by Means of  
451 Reflectance-Based Techniques. *Agron. J.* 100(5): 1409. doi: 10.2134/agronj2007.0322
- 452 Curran, P.J., and E.J. Milton. 1983. The relationships between the chlorophyll concentration,  
453 LAI and reflectance of a simple vegetation canopy. *Int. J. Remote Sens.* 4(2): 247-255. doi:  
454 10.1080/01431168308948544
- 455 Curran, P.J., and M.D. Steven. 1983. Multispectral Remote Sensing for the Estimation of Green  
456 Leaf Area Index [and Discussion]. *Philos. T. R. Sco. A.* 309(1508): 257-270. doi:  
457 10.1098/rsta.1983.0039
- 458 Dash, J., and P.J. Curran. 2004. The MERIS terrestrial chlorophyll index. *Int. J. Remote Sens.*  
459 25(23): 5403-5413. doi: 10.1080/0143116042000274015
- 460 Dash, J., and P.J. Curran. 2007. Evaluation of the MERIS terrestrial chlorophyll index (MTCI).  
461 *Adv. Space Res.* 39(1): 100-104. doi: 10.1016/j.asr.2006.02.034

- 462 Daughtry, C.S.T., C.L. Walthall, M.S. Kim, E. Brown de Colstoun, and J.E. McMurtrey III.  
463 2000. Estimating Corn Leaf Chlorophyll Concentration from Leaf and Canopy Reflectance.  
464 Remote Sens. Environ. 74(2): 229-239. doi: 10.1016/S0034-4257(00)00113-9
- 465 Doraiswamy, P.C., Moulin, S., and Cook, P.W. 2003. Crop yield assessment from remote  
466 sensing. Photogramm. Eng. Rem. S. 69: 665–674. doi: 10.1016/S0034-4257(00)00113-9
- 467 Ehleringer, J., and I. Forseth. 1980. Solar tracking by plants. Science. 210(4474): 1094-8. doi:  
468 10.1126/science.210.4474.1094
- 469 Eitel, J.U.H., D.S. Long, P.E. Gessler, E.R. Hunt, and D.J. Brown. 2009. Sensitivity of Ground-  
470 Based Remote Sensing Estimates of Wheat Chlorophyll Content to Variation in Soil  
471 Reflectance. Soil. Sci. Soc. Am. J. 73(5): 1715. doi: 10.2136/sssaj2008.0288
- 472 Eitel, J.U.H., D.S. Long, P.E. Gessler, and E.R. Hunt. 2008. Combined Spectral Index to  
473 Improve Ground-Based Estimates of Nitrogen Status in Dryland Wheat. Agron. J. 100(6):  
474 1694. doi: 10.2134/agronj2007.0362
- 475 Fang, H., S. Liang, and G. Hoogenboom. 2011. Integration of MODIS LAI and vegetation index  
476 products with the CSM-CERES-Maize model for corn yield estimation. Int. J. Remote Sens.  
477 32(4): 1039-1065. doi: 10.1080/01431160903505310
- 478 Gao, X., A.R. Huete, W. Nif, and T. Miura. 2000. Optical–Biophysical Relationships of  
479 Vegetation Spectra without Background Contamination. Remote Sens. Environ. 74(3): 609-  
480 620. doi: 10.1016/S0034-4257(00)00150-4
- 481 Gitelson, A.A. 2004. Wide Dynamic Range Vegetation Index for remote quantification of  
482 biophysical characteristics of vegetation. J. Plant Physiol. 161(2): 165-73. doi:  
483 10.1078/0176-1617-01176
- 484 Gitelson, A.A. 2011. Remote sensing estimation of crop biophysical characteristics at various  
485 scales. p. 1-36. In Thenkabail, P.S., Lyon, J.G., and Huete, A. (Ed.), Hyperspectral Remote  
486 Sensing of Vegetation. Taylor & Francis.
- 487 Gitelson, A.A., and M.N. Merzlyak. 1994. Spectral reflectance changes associated with autumn  
488 senescence of *Aesculus hippocastanum* L. and *Acer platanoides* L. leaves. Spectral features  
489 and relation to chlorophyll estimation. J. Plant Physiol. 143: 286–286. doi: 10.1016/S0176-  
490 1617(11)81633-0
- 491 Gitelson, A.A., Y. Gritz, and M.N. Merzlyak. 2003a. Relationships between leaf chlorophyll  
492 content and spectral reflectance and algorithms for non-destructive chlorophyll assessment  
493 in higher plant leaves. J. Plant Physiol. 160(3): 271-82. doi: 10.1078/0176-1617-00887
- 494 Gitelson, A.A., Y.J. Kaufman, and M.N. Merzlyak. 1996. Use of a green channel in remote  
495 sensing of global vegetation from EOS-MODIS. Remote Sens. Environ. 58(3): 289-298.  
496 doi: 10.1016/S0034-4257(96)00072-7

- 497 Gitelson, A.A., A. Viña, T.J. Arkebauer, D.C. Rundquist, G.P. Keydan, and B. Leavitt. 2003b.  
 498 Remote estimation of leaf area index and green leaf biomass in maize canopies. *Geophys.*  
 499 *Res. Lett.* 30(5): 1248. doi: 10.1029/2002GL016450
- 500 Gitelson, A.A., A. Viña, V. Ciganda, D.C. Rundquist, and T.J. Arkebauer. 2005. Remote  
 501 estimation of canopy chlorophyll content in crops. *Geophys. Res. Lett.* 32(8): L08403. doi:  
 502 10.1029/2005GL022688
- 503 Gitelson, A.A., B.D. Wardlow, G.P. Keydan, and B. Leavitt. 2007. An evaluation of MODIS  
 504 250-m data for green LAI estimation in crops. *Geophys. Res. Lett.* 34(20): L20403. doi:  
 505 10.1029/2007GL031620
- 506 Gobron, N., B. Pinty, M.M. Verstraete, and Y. Govaerts. 1997. A semidiscrete model for the  
 507 scattering of light by vegetation. *J. Geophys. Res.* 102(D8): 9431-9446. doi:  
 508 10.1029/96JD04013
- 509 González-Sanpedro, M.C., T. Le Toan, J. Moreno, L. Kergoat, and E. Rubio. 2008. Seasonal  
 510 variations of leaf area index of agricultural fields retrieved from Landsat data. *Remote Sens.*  
 511 *Environ.* 112: 810-824. doi: 10.1016/j.rse.2007.06.018
- 512 Govaerts, Y.M., M.M. Verstraete, B. Pinty, and N. Gobron. 1999. Designing optimal spectral  
 513 indices: A feasibility and proof of concept study. *Int. J. Remote Sens.* 20(9): 1853-1873.  
 514 doi: 10.1080/014311699212524
- 515 Guindin-Garcia, N., A.A. Gitelson, T.J. Arkebauer, J. Shanahan, A. Weiss. 2012. An evaluation  
 516 of MODIS 8- and 16-day composite products for monitoring maize green leaf area index.  
 517 *Ag. Forest Meterol.* 161: 15-25. doi:10.1016/j.agrformet.2012.03.012
- 518 Haboudane, D., J.R. Miller, E. Pattey, P.J. Zarco-Tejada, and I.B. Strachan. 2004. Hyperspectral  
 519 vegetation indices and novel algorithms for predicting green LAI of crop canopies:  
 520 Modeling and validation in the context of precision agriculture. *Remote Sens. Environ.*  
 521 90(3): 337-352. doi: 10.1016/j.rse.2003.12.013
- 522 Haboudane, D., J.R. Miller, N. Tremblay, P.J. Zarco-Tejada, and L. Dextraze. 2002. Integrated  
 523 narrow-band vegetation indices for prediction of crop chlorophyll content for application to  
 524 precision agriculture. *Remote Sens. Environ.* 81(2-3): 416-426. doi: 10.1016/S0034-  
 525 4257(02)00018-4
- 526 Hatfield, J.L., Prueger, J.H., and Kustas, W.P. Remote sensing of dryland crops. pp. 531–568,  
 527 2004. *In:* Ustin, S.L. (ed.), *Remote Sensing for Natural Resource Management and*  
 528 *Environmental Monitoring: Manual of Remote Sensing.* 3rd Edition. Hoboken, NJ.
- 529 Hatfield, J.L., Gitelson, A.A., Schepers, J.S., and Walthall, C.L. 2008. Application of spectral  
 530 remote sensing for agronomic decisions. *Agron. J.* 100: S-117–131.  
 531 doi:10.2134/agronj2006.0370c

- 532 Huete, A.R., K. Didan, T. Miura, E. Rodriguez, X. Gao, and L. Ferreira. 2002. Overview of the  
533 radiometric and biophysical performance of the MODIS vegetation indices. *Remote Sens.*  
534 *Environ.* 83(1-2): 195-213. doi: 10.1016/S0034-4257(02)00096-2
- 535 Huete, A.R., H.Q. Liu, K. Batchily, and W. van Leeuwen. 1997. A comparison of vegetation  
536 indices over a global set of TM images for EOS-MODIS. *Remote Sens. Environ.* 59(3):  
537 440-451. doi: 10.1016/S0034-4257(96)00112-5
- 538 Idso, S.B., and C.T. de Wit. 1970. Light relations in plant canopies. *Appl. Optics* 9(1): 177-84.  
539 doi: 10.1364/AO.9.000177
- 540 Jiang, Z., A.R. Huete, K. Didan, and T. Miura. 2008. Development of a two-band enhanced  
541 vegetation index without a blue band. *Remote Sens. Environ.* 112: 3833-3845. doi:  
542 10.1016/j.rse.2008.06.006
- 543 Jordan, C.F. 1969. Derivation of Leaf-Area Index from Quality of Light on the Forest Floor.  
544 *Ecology* 50(4): 663-666. doi: 10.2307/1936256
- 545 Kanemasu, E.T. 1974. Seasonal canopy reflectance patterns of wheat, sorghum, and soybean.  
546 *Remote Sens. Environ.* 3(1): 43-47. doi: 10.1016/0034-4257(74)90037-6
- 547 Kohavi, R. 1995. A Study of Cross-Validation and Bootstrap for Accuracy Estimation and  
548 Model Selection. p. 1137-1143. *In* Mellish, C.S. (ed.), *International joint conference on*  
549 *artificial intelligence*. Montreal, Quebec, Canada.
- 550 le Maire, G., François, C., Soudani, K., Berveiller, D., Pontailier, J.Y., and Bréda, N. 2008.  
551 Calibration and validation of hyperspectral indices for the estimation of broadleaved forest  
552 leaf chlorophyll content, leaf mass per area, leaf area index and leaf canopy biomass.  
553 *Remote Sens. Environ.* 112, 3846–3864. doi: 10.1016/j.rse.2008.06.005
- 554 Liu, H.Q., and A.R. Huete. 1995. A feedback based modification of the NDVI to minimize  
555 canopy background and atmospheric noise. *IEEE T. Geosci. Remote* 33(2): 457-465. doi:  
556 10.1109/36.377946
- 557 Myneni, R.B., F.G. Hall, P.J. Sellers, and A.L. Marshak. 1995. The interpretation of spectral  
558 vegetation indexes. *IEEE T. Geosci. Remote* 33(2): 481-486. doi: 10.1109/36.377948
- 559 Pinter, P.J., Hatfield, J.L., Schepers, J.S., Barnes, E.M., Moran, M.S., Daughtry, C.S., and  
560 Upchurch, D.R. 2003. Remote sensing for crop management. *Photogramm. Eng. Rem. S.*  
561 69, 647–664. doi: 10.1109/IGARSS.2007.4423218
- 562 Peng, Y., and A.A. Gitelson. 2011. Application of chlorophyll-related vegetation indices for  
563 remote estimation of maize productivity. *Ag. Forest Meteorol.* 151(9): 1267-1276. doi:  
564 10.1016/j.agrformet.2011.05.005

- 565 Peng, Y., A.A. Gitelson, G.P. Keydan, D.C. Rundquist, and W. Moses. 2011. Remote estimation  
566 of gross primary production in maize and support for a new paradigm based on total crop  
567 chlorophyll content. *Remote Sens. Environ.* 115(4): 978-989. doi:  
568 10.1016/j.rse.2010.12.001
- 569 Ritz, C., and J.C. Streibig. 2008. Grouped Data. p. 109-131. *In* Ritz, C., Streibig, J.C. (eds.),  
570 *Nonlinear Regression with R*. Springer Science+Business Media, LLC, New York, NY.
- 571 Rondeaux, G., M. Steven, and F. Baret. 1996. Optimization of soil-adjusted vegetation indices.  
572 *Remote Sens. Environ.* 55(2): 95-107. doi: 10.1016/0034-4257(95)00186-7
- 573 Rouse, J.W., R.H. Haas, J.A. Schell, and D.W. Deering. 1973. Monitoring vegetation systems in  
574 the Great Plains with ERTS. p. 309-317. *In* Freden, S.C., Becker, M.A. (eds.), *Third ERTS*  
575 *Symposium*. NASA.
- 576 Rundquist, D.C., R. Perk, B. Leavitt, G.P. Keydan, and A.A. Gitelson. 2004. Collecting spectral  
577 data over cropland vegetation using machine-positioning versus hand-positioning of the  
578 sensor. *Comput. Electron. Agr.* 43(2): 173-178. doi: 10.1016/j.compag.2003.11.002
- 579 Schmidt, M., and H. Lipson. 2009. Distilling free-form natural laws from experimental data.  
580 *Science* 324(5923): 81-5. doi: 10.1126/science.116589
- 581 Smith, A.M., G. Bourgeois, P.M. Teillet, J. Freemantle, and C. Nadeau. 2008. A comparison of  
582 NDVI and MTVI2 for estimating LAI using CHRIS imagery: a case study in wheat. *Can. J.*  
583 *Remote Sens.* 34(6): 539-548. doi: 10.5589/m08-071
- 584 Suyker, A.E., and S.B. Verma. 2010. Coupling of carbon dioxide and water vapor exchanges of  
585 irrigated and rainfed maize–soybean cropping systems and water productivity. *Ag. Forest*  
586 *Meterol.* 150(4): 553-563. doi: 10.1016/j.agrformet.2010.01.020
- 587 Suyker, A.E., S.B. Verma, G. Burba, T.J. Arkebauer, D.T. Walters, and K.G. Hubbard. 2004.  
588 Growing season carbon dioxide exchange in irrigated and rainfed maize. *Ag. Forest*  
589 *Meterol.* 124(1-2): 1-13. doi: 10.1016/j.agrformet.2004.01.011
- 590 Verma, S.B., A. Dobermann, K.G. Cassman, D.T. Walters, J.M. Knops, T.J. Arkebauer, A.E.  
591 Suyker, G.G. Burba, B. Amos, H. Yang, D. Ginting, K.G. Hubbard, A.A. Gitelson, and E.A.  
592 Walter-Shea. 2005. Annual carbon dioxide exchange in irrigated and rainfed maize-based  
593 agroecosystems. *Ag. Forest Meterol.* 131(1-2): 77-96. doi: 10.1016/j.agrformet.2005.05.003
- 594 Viña, A., and A.A. Gitelson. 2005. New developments in the remote estimation of the fraction of  
595 absorbed photosynthetically active radiation in crops. *Geophys. Res. Lett.* 32(17): L17403.  
596 doi: 10.1029/2005GL023647
- 597 Viña, A., A.A. Gitelson, A.L. Nguy-Robertson, and Y. Peng. 2011. Comparison of different  
598 vegetation indices for the remote assessment of green leaf area index of crops. *Remote*  
599 *Sens. Environ.* 115(12): 3468-3478. doi: 10.1016/j.rse.2011.08.010,



- 600 Wang, Q., S. Adiku, J. Tenhunen, and A. Granier. 2005. On the relationship of NDVI with leaf  
601 area index in a deciduous forest site. *Remote Sens. Environ.* 94(2): 244-255. doi:  
602 10.1016/j.rse.2004.10.006
- 603 Watson, D.J. 1947. Comparative physiological studies on the growth of field crops: I. Variation  
604 in net assimilation rate and leaf area between species and varieties, and within and between  
605 years. *Ann. Bot. London* 11(1): 41-76.
- 606 de Wit, C.T. 1965. Photosynthesis of leaf canopies. *Agric. Res. Rep.*663. Inst. For Biol. And  
607 Chem. Res. On Field Crops and Herbage, Wageningen, the Netherlands.
- 608 Wu, J., D. Wang, and M. Bauer. 2007. Assessing broadband vegetation indices and QuickBird  
609 data in estimating leaf area index of corn and potato canopies. *Field Crop Res.* 102(1): 33-  
610 42. doi: 10.1016/j.fcr.2007.01.003

611

612 Fig. 1: Temporal dynamics of gLAI in a) maize in 2007 and b) soybean in 2008, in both irrigated  
 613 (solid line) and rainfed (dashed line) fields. Major crop growth stages (vegetative, reproductive,  
 614 and senescence) are indicated. Bars represent one standard error of destructive gLAI  
 615 determination at six intensive measurement zones in each field.

616 Fig. 2: Vegetation indices plotted versus green leaf area index, gLAI: a) Simple Ratio, b)  
 617 Normalized Difference Vegetation Index (NDVI), c) green NDVI, d) red edge NDVI, e)  
 618 Optimized Soil-Adjusted Vegetation Index (OSAVI), f) Chlorophyll Index Green ( $CI_{green}$ ), g)  
 619  $CI_{red\ edge}$ , h) Triangular Vegetation Index (TVI), i) MERIS Terrestrial Chlorophyll Index  
 620 (MTCI), j) Wide Dynamic Range Vegetation Index (WDRVI)  $\alpha=0.2$ , k) Modified TVI 2  
 621 (MTVI2), and l) Enhanced Vegetation Index 2 (EVI2). In all panels – maize: open squares, solid  
 622 line is best-fit function; soybean: closed triangles, dashed line is best fit function. The inverse of  
 623 these relationships gLAI vs. VIs along with their summary statistics are shown in Tables 3 and 4.  
 624

625 Fig. 3: Minimal and maximal values of the noise equivalent NE  $\Delta gLAI$  for a) maize and b)  
 626 soybean for groupings of vegetation indices demonstrating increase of NE (decrease in accuracy)  
 627 at moderate-to-high gLAI (NDVI, green NDVI, red edge NDVI, OSAVI, and WDRVI), high NE  
 628 at low-to-moderate gLAI (SR,  $CI_{green}$  and  $CI_{red\ edge}$ ) and almost invariant NE throughout the  
 629 entire dynamic range (MTCI).

630  
 631 Fig. 4: Noise equivalent NE  $\Delta gLAI$  of NDVI, SR and suggested combined vegetation index  
 632  $CVI\{NDVI, SR\}$  for (a) maize and (b) soybean. NDVI < 0.7 is the first index and SR is the  
 633 second index.

634 Fig. 5: Noise equivalent NE  $\Delta gLAI$  of red edge NDVI,  $CI_{red\ edge}$  and suggested combined  
 635 vegetation index  $CVI\{red\ edge\ NDVI, CI_{red\ edge}\}$  for maize and soybean combined. Red edge  
 636 NDVI < 0.6 is the first index and  $CI_{red\ edge}$  is the second index.

637

638 Table 1: Species, hybrid, planting density and maximum green leaf area index (gLAI) in the 24  
 639 year-fields evaluated.

Year	Site	Species	Hybrid	Planting Density (pl/ha)	Maximum gLAI (m <sup>2</sup> /m <sup>2</sup> )	Tillage operation	Applied N
2001	1	maize	Pioneer 33P67	82,000	6.1	intensive tillage	196
	2	maize	Pioneer 33P67	83,314	6.1		196
	3	maize	Pioneer 33B51	62,236	3.9		128
2002	1	maize	Pioneer 33P67	81,000	6.0	no-till	214
	2	soybean	Asgrow 2703	370,644	5.5		0
	3	soybean	Asgrow 2703	370,644	3.0		0
2003	1	maize	Pioneer 33B51	77,000	5.5	no-till	233
	2	maize	Pioneer 33B51	86,667	5.5		169
	3	maize	Pioneer 33B51	64,292	4.3		90
2004	1	maize	Pioneer 33B51	84,012	5.2	no-till	293
	2	soybean	Pioneer 93B09	370,644	4.4		0
	3	soybean	Pioneer 93B09	370,644	4.5		0
2005	1	maize	DeKalb 63-75	82,374	5.2	no-till	246
	2	maize	Pioneer 33B51	83,200	4.8		170
	3	maize	Pioneer 33G68	59,184	4.3		118
2006	1	maize	Pioneer 33B53	84,012	5.3	conservation-plow	210
	2	soybean	Pioneer 31N28	370,644	5.0	no-till	0
	3	soybean	Pioneer 93M11	370,644	4.5		0
2007	1	maize	Pioneer 31N30	80,697	6.3	conservation-plow	272
	2	maize	Pioneer 31N28	78,740	5.7	no-till	183
	3	maize	Pioneer 33H26	62,088	4.1		125
2008	1	maize	Pioneer 31N30	84,469	6.5	conservation-plow	123
	2	soybean	Pioneer 93M11	369,508	4.7	no-till	0
	3	soybean	Pioneer 93M11	369,508	3.6		0

640  
 641

642 Table 2: List and formulation of the vegetation indices examined.

Index	Equation	Equation in Bands of MODIS or/and MERIS	Reference
Simple Ratio (SR)	NIR/Red	MODIS 2 / MODIS 1	Jordan, (1969)
Normalized Difference Vegetation Index (NDVI)	$(\text{NIR} - \text{Red}) / (\text{NIR} + \text{Red})$	$(\text{MODIS 2} - \text{MODIS 1}) / (\text{MODIS 2} + \text{MODIS 1})$	Rouse et al., (1973)
Green NDVI (green NDVI)	$(\text{NIR} - \text{Green}) / (\text{NIR} + \text{Green})$	$(\text{MODIS 2} - \text{MODIS 4}) / (\text{MODIS 2} + \text{MODIS 4})$	Gitelson and Merzlyak, (1994)
Red Edge NDVI (red edge NDVI)	$(\text{NIR} - \text{Red Edge}) / (\text{NIR} + \text{Red Edge})$	$(\text{MERIS 12} - \text{MERIS 9}) / (\text{MERIS 12} + \text{MERIS 9})$	Gitelson and Merzlyak, (1994)
Optimized Soil-Adjusted Vegetation Index (OSAVI)	$(\text{NIR} - \text{Red}) / (\text{Red} + \text{NIR} + 0.16)$	$(\text{MODIS 2} - \text{MODIS 1}) / (\text{MODIS 1} + \text{MODIS 2} + 0.16)$	Rondeaux et al., (1996)
Green Chlorophyll Index ( $\text{CI}_{\text{green}}$ )	$(\text{NIR} / \text{Green}) - 1$	$(\text{MODIS 2} / \text{MODIS 4}) - 1$	Gitelson et al., (1996)
Red Edge Chlorophyll Index ( $\text{CI}_{\text{red edge}}$ )	$(\text{NIR} / \text{Red Edge}) - 1$	$(\text{MERIS 12} / \text{MERIS 9}) - 1$	Gitelson et al., (1996)
Triangular Vegetation Index (TVI)	$0.5 * [120 * (\text{NIR} - \text{Green}) - 200 * (\text{Red} - \text{Green})]$	$0.5 * [120 * (\text{MERIS 10} - \text{MERIS 5}) - 200 * (\text{MERIS 7} - \text{MERIS 5})]$	Broge and Leblanc, (2001)
MERIS Terrestrial Chlorophyll Index (MTCI)	$(\text{NIR} - \text{Red Edge}) / (\text{Red Edge} - \text{Red})$	$(\text{MERIS 10} - \text{MERIS 9}) / (\text{MERIS 9} + \text{MERIS 8})$	Dash and Curran, (2004)
Wide Dynamic Range Vegetation Index <sup>#</sup>	$(\alpha * \text{NIR} - \text{Red}) / (\alpha * \text{NIR} + \text{Red})$	$(\alpha * \text{MODIS 2} - \text{MODIS 1}) / (\alpha * \text{MODIS 2} + \text{MODIS 1})$	Gitelson, (2004)
Modified TVI 2 (MTVI2)	$1.5 * [1.2 * (\text{NIR} - \text{Green}) - 2.5 * (\text{Red} - \text{Green})] / \sqrt{\{2 * \text{NIR} + 1\}^2 - [6 * \text{NIR} - 5 * \sqrt{\text{Red}}] - 0.5}$	$1.5 * [1.2 * (\text{MODIS 2} - \text{MODIS 4}) - 2.5 * (\text{MODIS 1} - \text{MODIS 4})] / \sqrt{\{2 * \text{MODIS 2} + 1\}^2 - [6 * \text{MODIS 2} - 5 * \sqrt{\text{MODIS 1}}] - 0.5}$	Haboudane et al., (2004)
Enhanced Vegetation Index 2 (EVI2)	$2.5 * (\text{NIR} - \text{Red}) / (\text{NIR} + 2.4 * \text{Red} + 1)$	$2.5 * (\text{MODIS 2} - \text{MODIS 1}) / (\text{MODIS 2} + 2.4 * \text{MODIS 1} + 1)$	(Jiang et al., (2008)

643 <sup>#</sup>This study utilized scaled WDRVI in the form  $(\alpha * \text{MODIS Band 2} - \text{MODIS Band 1}) / (\alpha * \text{MODIS Band 2}$   
644  $+ \text{MODIS Band 1}) + (1 - \alpha) / (1 + \alpha)$  (Peng et al. 2011).

645 Table 3: Best-fit functions of the relationships between green leaf area index (gLAI) and  
 646 vegetation indices (VI) obtained using a cross-validation procedure for maize;  $x = VI$ ,  $y = gLAI$ ,  
 647  $R^2$  is the coefficient of determination, and the SE is the standard error of the gLAI estimation, in  
 648  $m^2/m^2$ .

Index	Equation gLAI vs VI	$R^2$	SE
SR	$y = x^{0.654} - 1.24$	0.86	0.66
NDVI	$y = \log_{0.6}[-(x - 0.943) / 0.731]$	0.87	0.64
Green NDVI	$y = -\{[\ln(0.876 - x) + 0.66] / 0.409\}$	0.87	0.63
Red edge NDVI	$y = \log_{0.716}(0.88 - x) - 0.623$	0.90	0.54
OSAVI	$y = -[1.49 * \ln(x) + 2.71] / \ln(x)$	0.81	0.78
$CI_{green}$	$y = [(x - 0.931) / 1.44]^{0.971}$	0.89	0.59
$CI_{red\ edge}$	$y = [(x - 0.15) / 0.642]^{0.775}$	0.90	0.55
TVI	$y = (x / 8.85)^{1.73}$	0.65	1.05
MTCI	$y = (x - 1.49)^{0.926}$	0.85	0.69
WDRVI $\alpha=0.2$	$y = \log_{0.775}(1.61 - x) + 1.61$	0.88	0.60
MTVI2	$y = \log_{0.81}(1.05 - x)$	0.67	1.01
EVI2	$y = (x + 0.863)^{4.08} - 0.863$	0.63	1.07

649

650

651

652 Table 4: Best-fit functions of the relationships between green leaf area index (gLAI) and  
 653 vegetation indices (VI) obtained using a cross-validation procedure for soybean;  $x = VI$ ,  $y =$   
 654 gLAI,  $R^2$  is the coefficient of determination, and the SE is the standard error of gLAI estimation,  
 655 in  $m^2/m^2$ .

Index	Equation gLAI vs VI	$R^2$	SE
SR	$y = [(x - 1.39)^{0.698}] / 2$	0.89	0.51
NDVI	$y = \log_{0.37}[x^{-0.526} - 1.03]$	0.90	0.48
Green NDVI	$y = \text{sqrt}[(0.964 - x)^{-1.48} - 2.35]$	0.89	0.51
Red edge NDVI	$y = \ln[(0.805 - x)^{(1/0.52)} - 0.82]$	0.91	0.46
OSAVI	$y = -[0.916 * \ln(1/x) - 1.79] / \ln(1/x)$	0.84	0.60
$CI_{\text{green}}$	$y = [(x - 1.08) / 1.38]^{0.767}$	0.90	0.49
$CI_{\text{red edge}}$	$y = (x / 0.86)^{0.854}$	0.91	0.46
TVI	$y = \exp(x / 17.2) - 1.06$	0.60	0.95
MTCI	$y = (x - 1.03)^{0.981}$	0.80	0.67
WDRVI $\alpha=0.2$	$y = -\{[\ln(1.79 - x) - 0.532] / 0.3\}$	0.90	0.47
MTVI2	$y = x^{1.61} / 0.172$	0.82	0.64
EVI2	$y = \exp(x / 0.472) - 1.3$	0.76	0.75

656

657

658 Table 5: Best-fit functions of the relationships between green leaf area index (gLAI) and  
 659 vegetation indices (VI) for both maize and soybean combined;  $x = VI$ ,  $y = gLAI$ ,  $R^2$  is the  
 660 coefficient of determination, and the SE is the standard error of the gLAI estimation, in  $m^2/m^2$ .  
 661

Index	Equation gLAI vs VI	$R^2$	SE
Red Edge NDVI	$y = (0.155 / x - 0.173)^{-0.542} - 0.739$	0.90	0.56
$CI_{red\ edge}$	$y = x^{0.898} / 0.904$	0.91	0.54

662

663

664 Table 6: Best-fit functions for combined vegetation indices (CVI) as used to estimate gLAI. CVI  
 665 represents the combination of two vegetation indices where the first index (i.e., NDVI or red  
 666 edge NDVI) are most sensitive to low-to-moderate gLAI and the second index (i.e., SR or  $CI_{red}$   
 667  $_{edge}$ ) are most sensitive to moderate-to-high gLAI. The threshold for NDVI was set at 0.7 and for  
 668 red edge NDVI at 0.6. CV is coefficient of variation.

<b>Index</b>	<b>Crop</b>	<b>First index below threshold</b>	<b>Second index above threshold</b>	<b>CV (%)</b>
CVI{NDVI, SR}	Maize	(NDVI - 0.28)/0.18	(SR + 1.0)/3.5	20
CVI{NDVI, SR}	Soybean	(NDVI - 0.27)/0.22	(SR + 3.2)/6.2	23
CVI{Red Edge NDVI, $CI_{red edge}$ }	Maize and Soybean	(red edge NDVI - 0.13)/0.14	( $CI_{red edge} - 0.63$ )/0.95	20

669

670

671

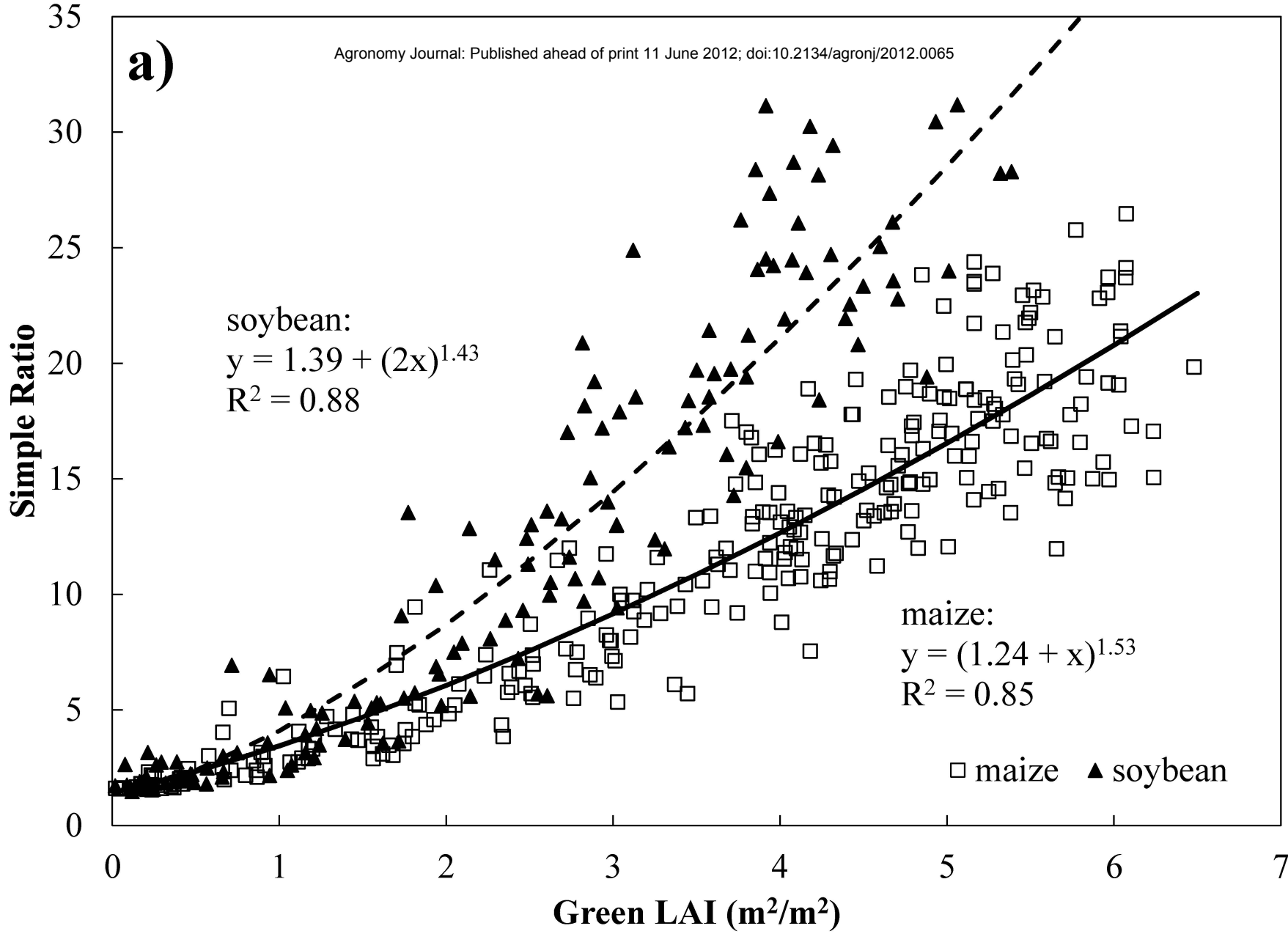


**a)**

soybean:  
 $y = 1.39 + (2x)^{1.43}$   
 $R^2 = 0.88$

maize:  
 $y = (1.24 + x)^{1.53}$   
 $R^2 = 0.85$

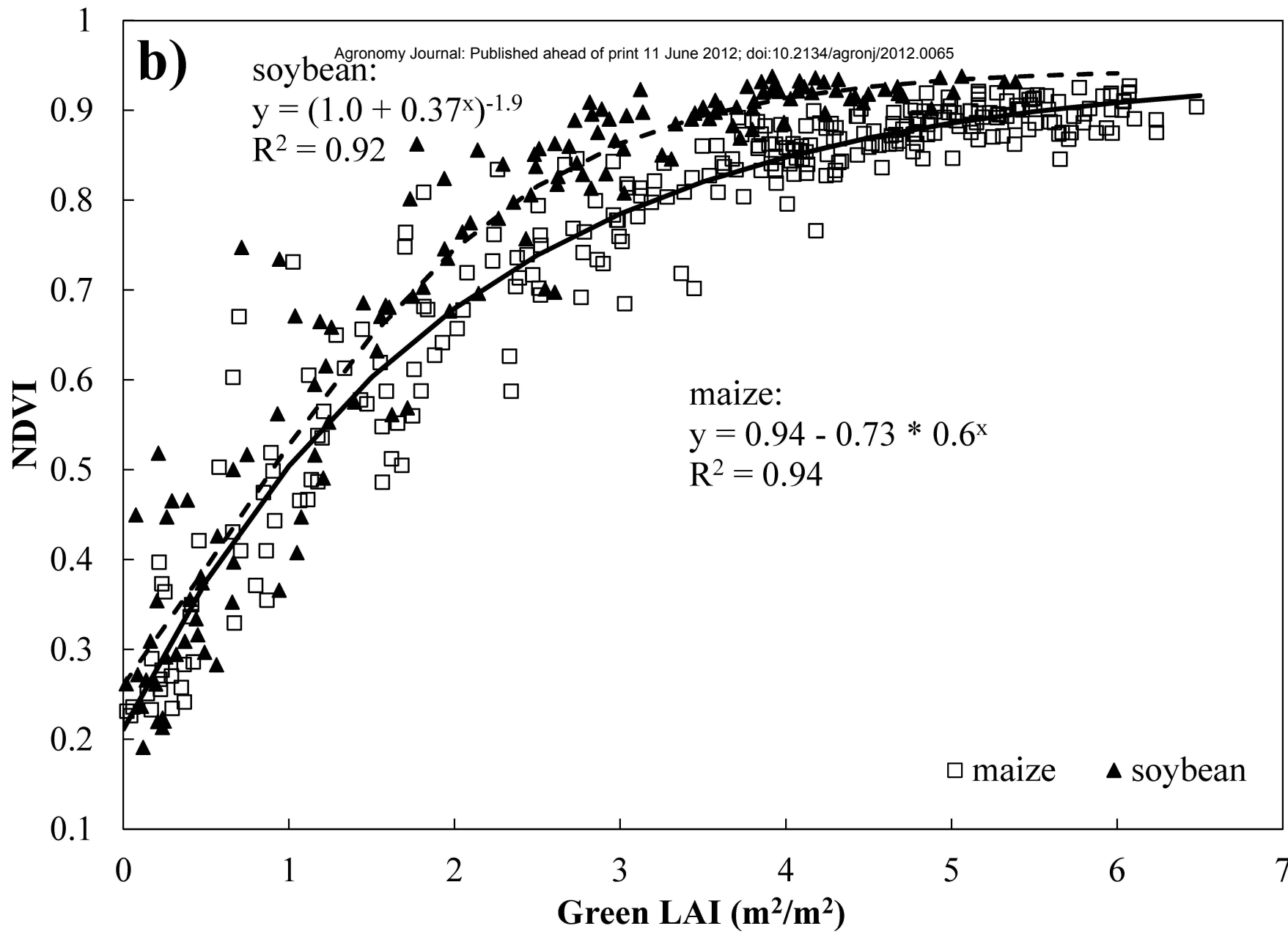
□ maize ▲ soybean



**b)**

soybean:  
 $y = (1.0 + 0.37^x)^{-1.9}$   
 $R^2 = 0.92$

maize:  
 $y = 0.94 - 0.73 * 0.6^x$   
 $R^2 = 0.94$



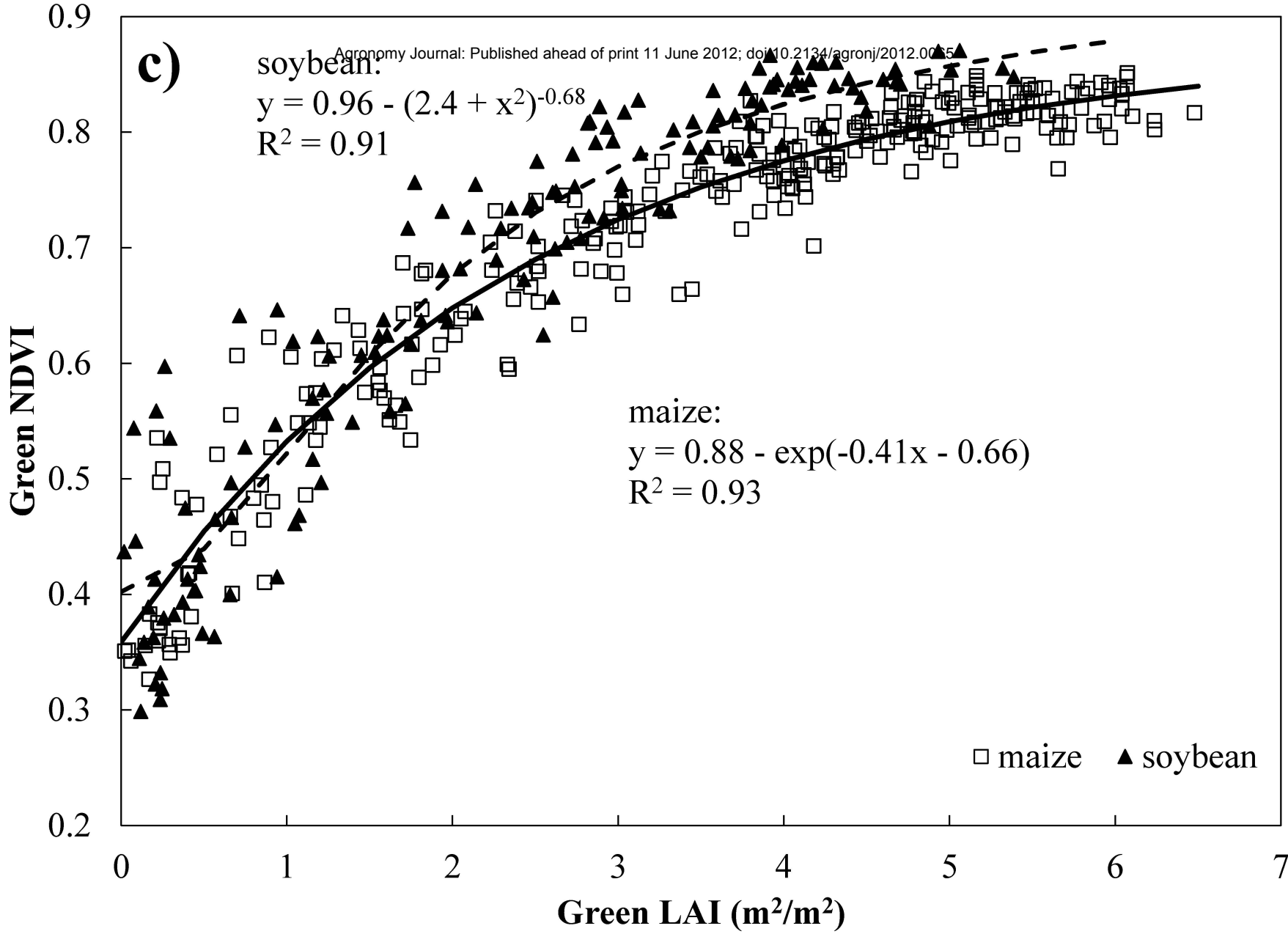
□ maize    ▲ soybean

c)

soybean:  
 $y = 0.96 - (2.4 + x^2)^{-0.68}$   
 $R^2 = 0.91$

maize:  
 $y = 0.88 - \exp(-0.41x - 0.66)$   
 $R^2 = 0.93$

□ maize ▲ soybean



d)

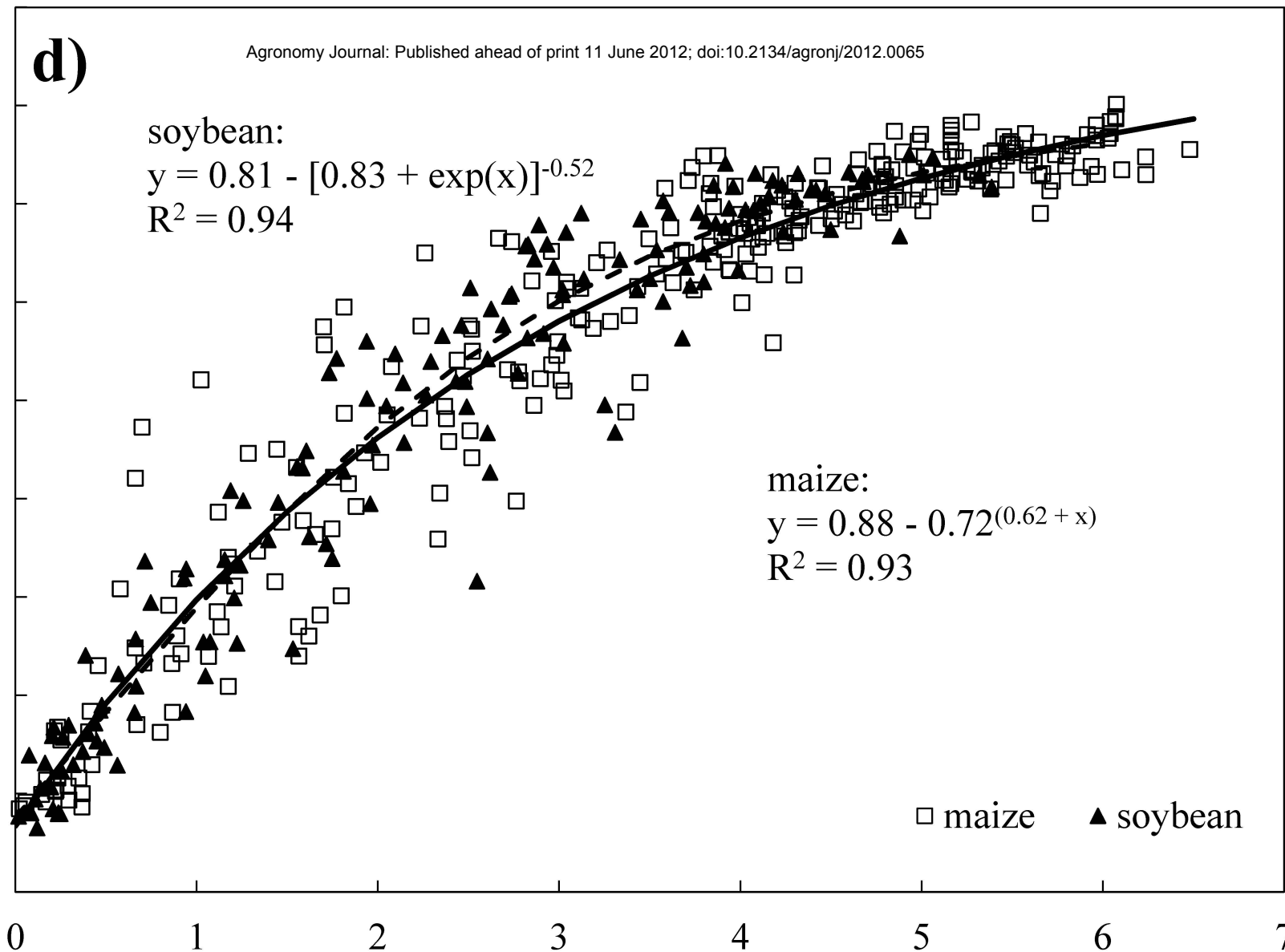
soybean:  
 $y = 0.81 - [0.83 + \exp(x)]^{-0.52}$   
 $R^2 = 0.94$

maize:  
 $y = 0.88 - 0.72^{(0.62 + x)}$   
 $R^2 = 0.93$

Red Edge NDVI

Green LAI ( $m^2/m^2$ )

□ maize    ▲ soybean



e)

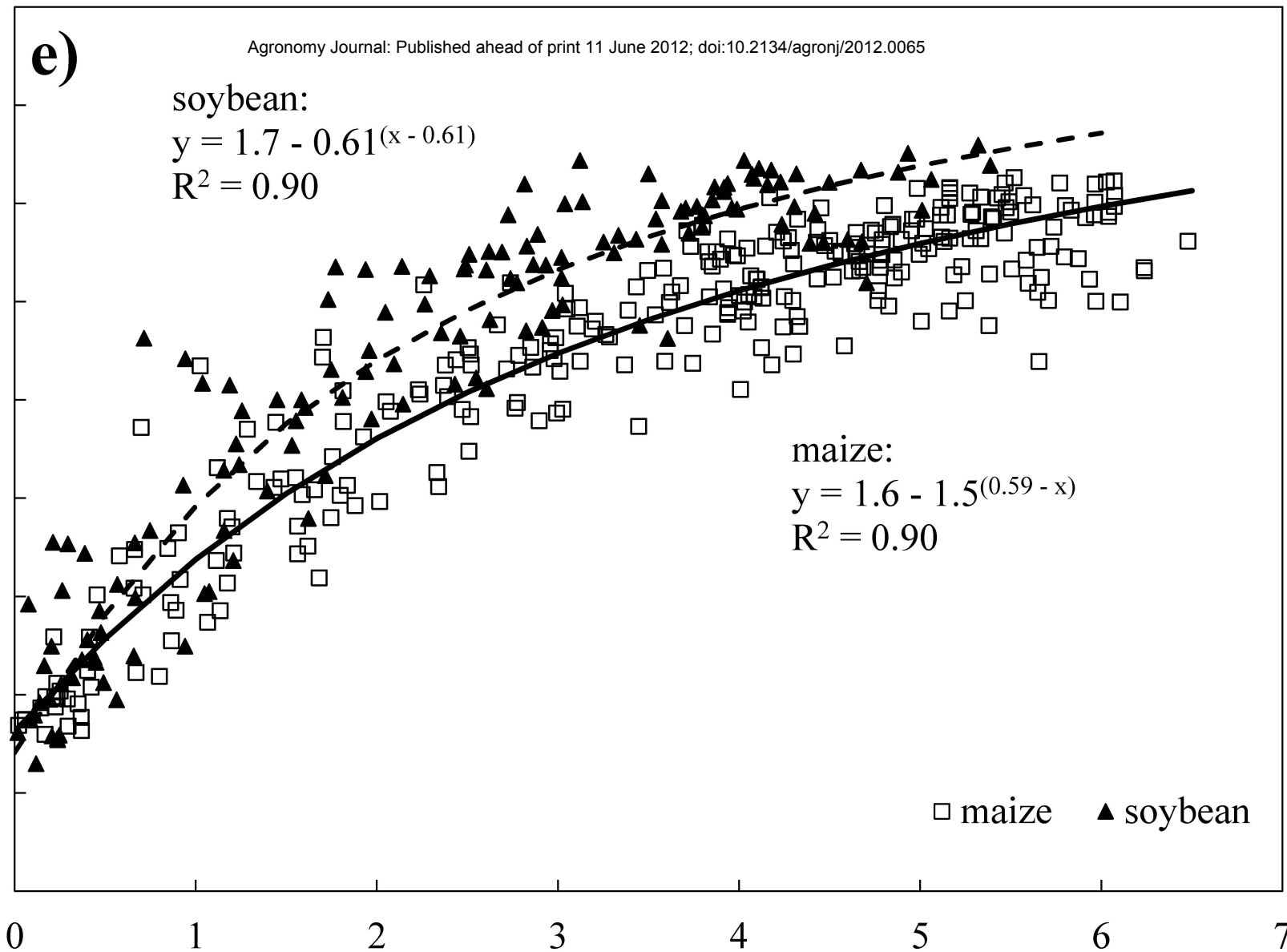
soybean:  
 $y = 1.7 - 0.61(x - 0.61)$   
 $R^2 = 0.90$

maize:  
 $y = 1.6 - 1.5(0.59 - x)$   
 $R^2 = 0.90$

□ maize ▲ soybean

OSAVI

Green LAI (m<sup>2</sup>/m<sup>2</sup>)

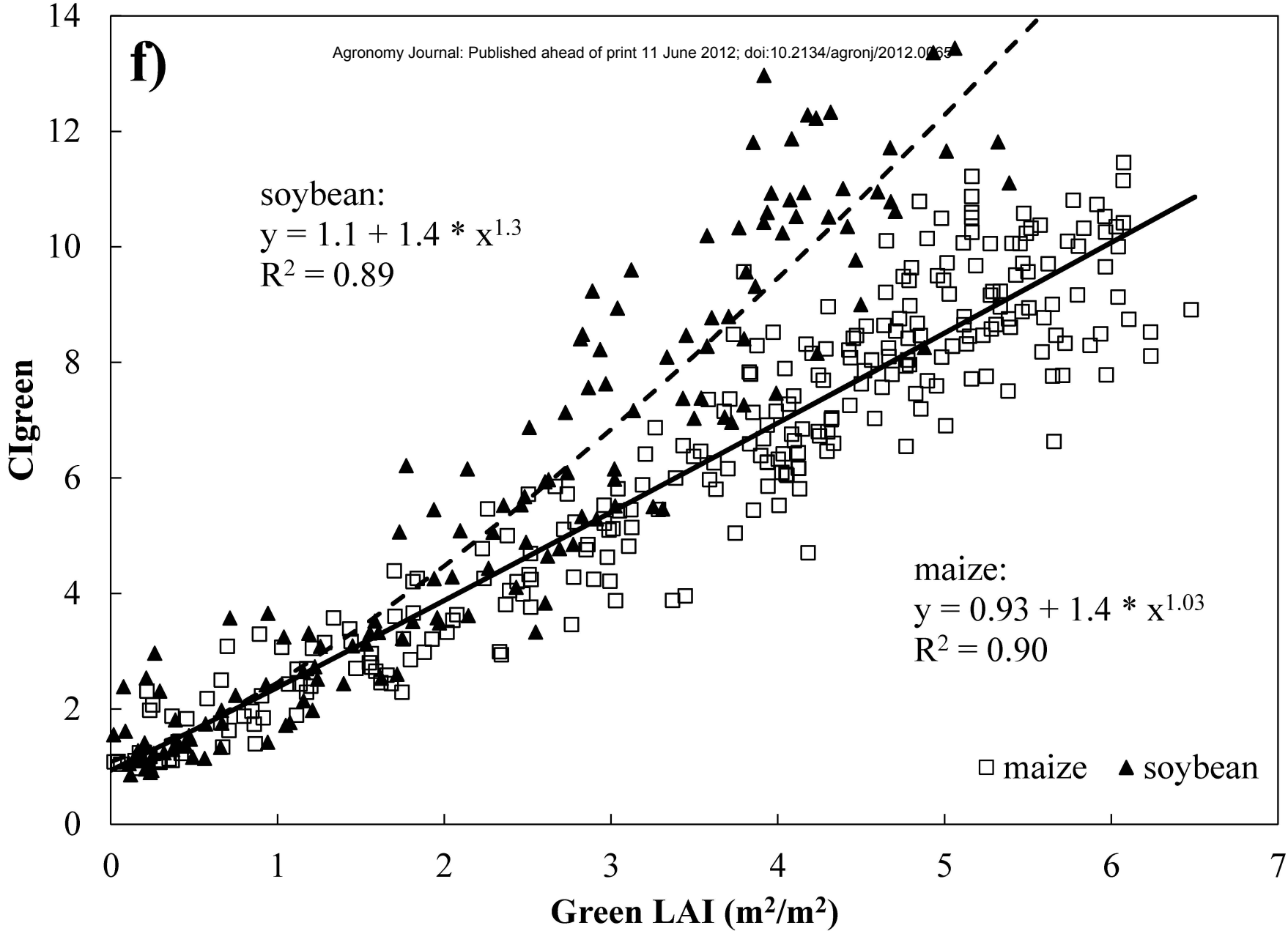


**f)**

soybean:  
 $y = 1.1 + 1.4 * x^{1.3}$   
 $R^2 = 0.89$

maize:  
 $y = 0.93 + 1.4 * x^{1.03}$   
 $R^2 = 0.90$

□ maize ▲ soybean

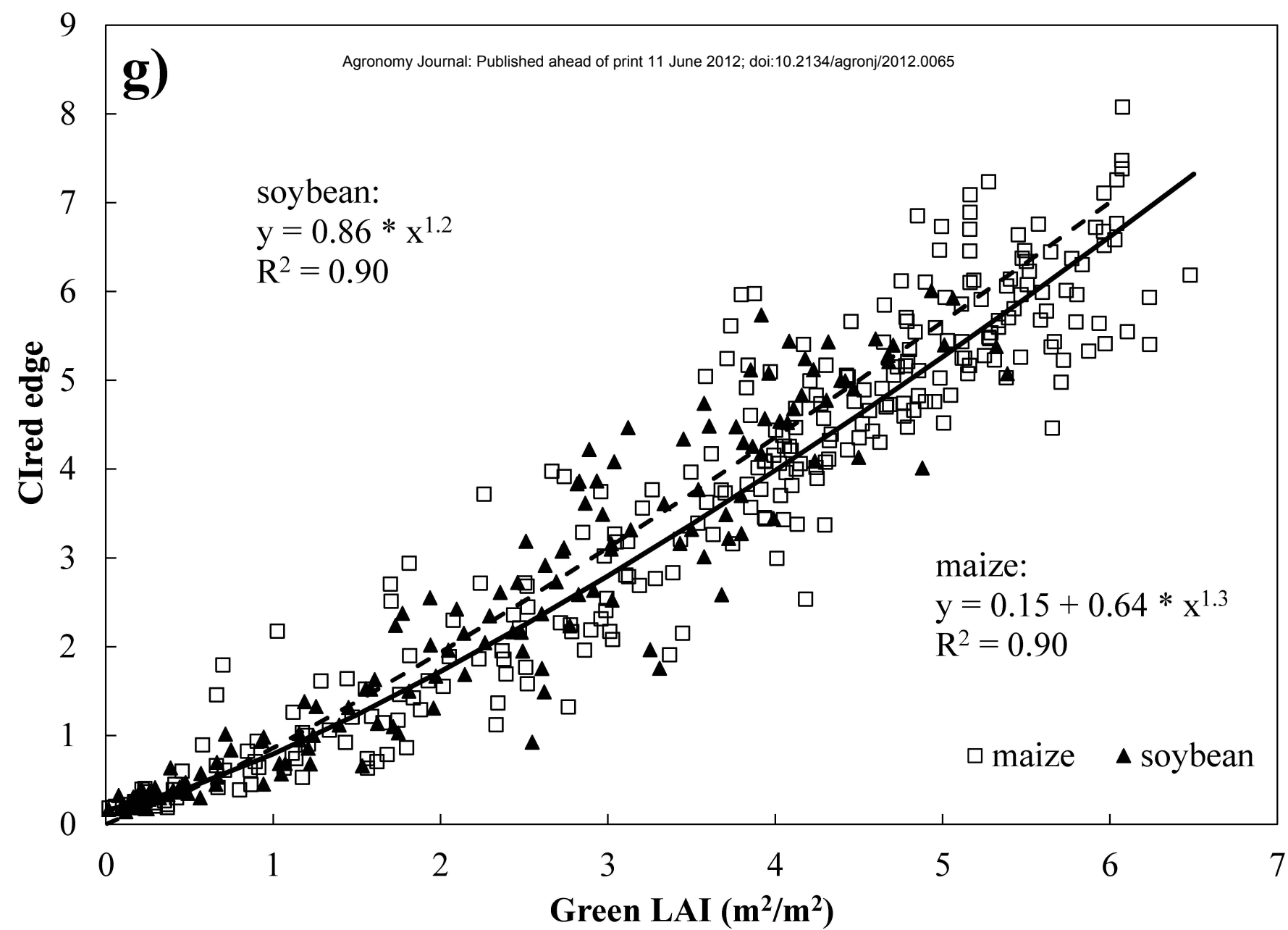


g)

soybean:  
 $y = 0.86 * x^{1.2}$   
 $R^2 = 0.90$

maize:  
 $y = 0.15 + 0.64 * x^{1.3}$   
 $R^2 = 0.90$

□ maize ▲ soybean

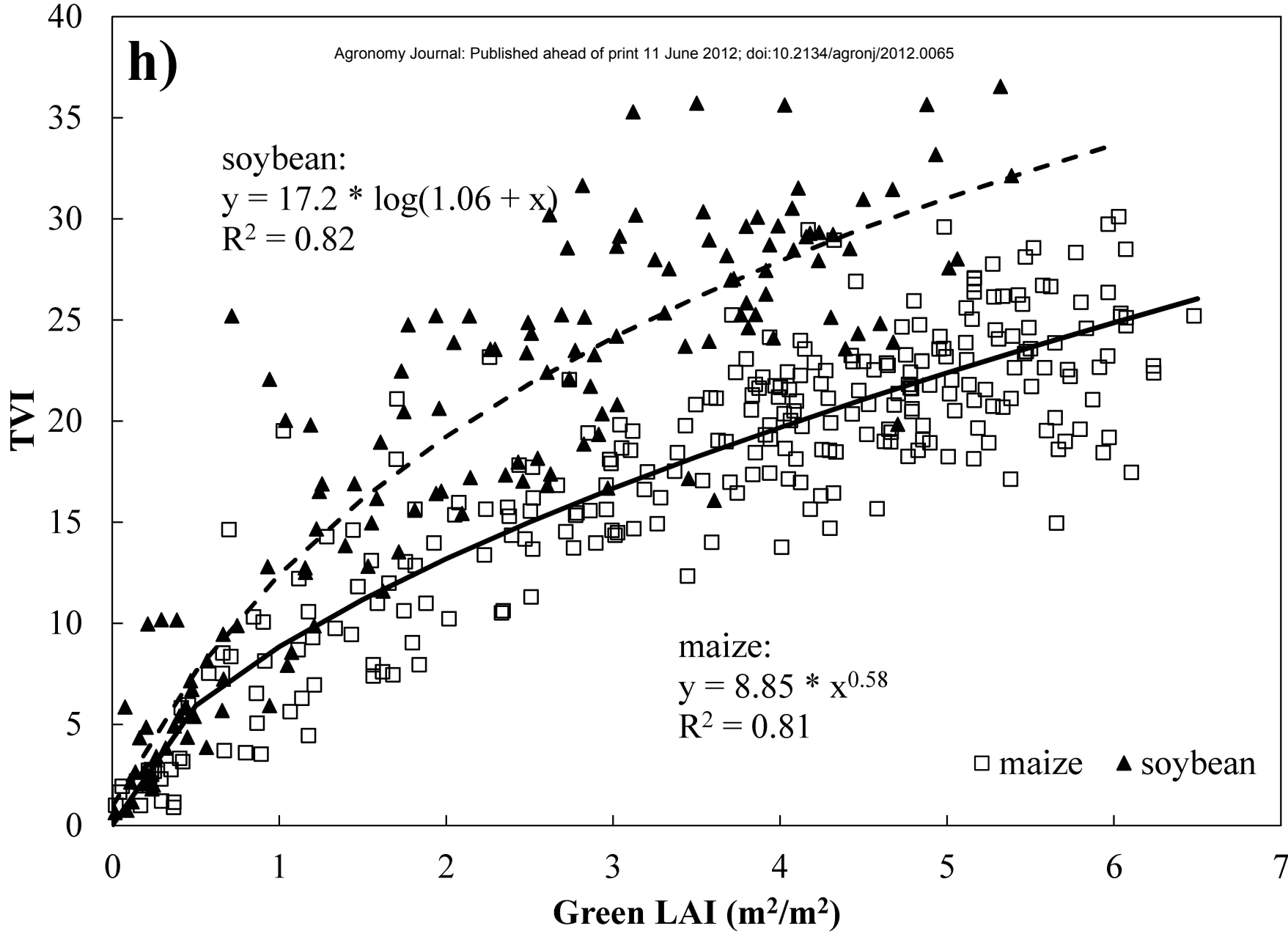


**h)**

soybean:  
 $y = 17.2 * \log(1.06 + x)$   
 $R^2 = 0.82$

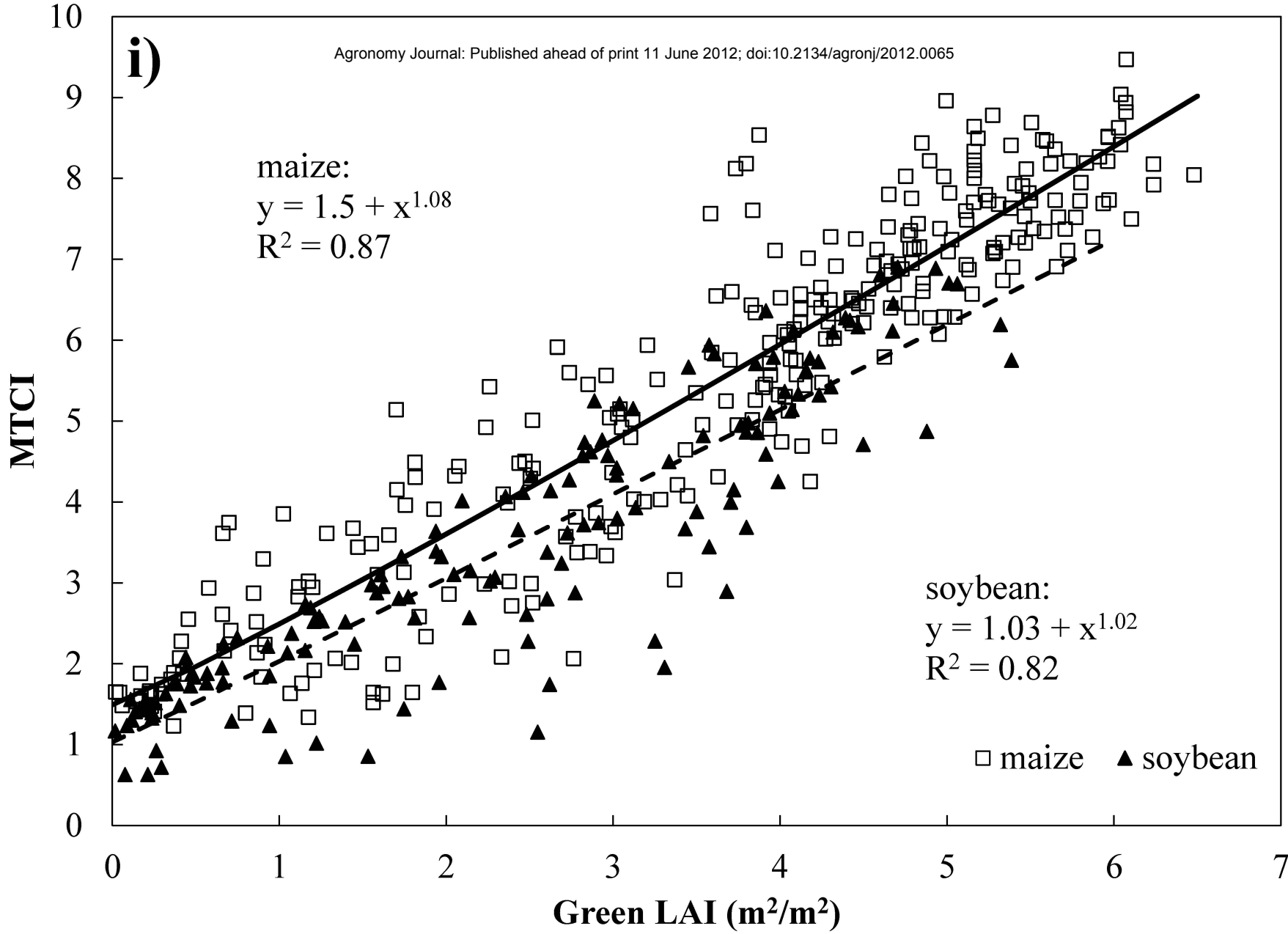
maize:  
 $y = 8.85 * x^{0.58}$   
 $R^2 = 0.81$

□ maize    ▲ soybean





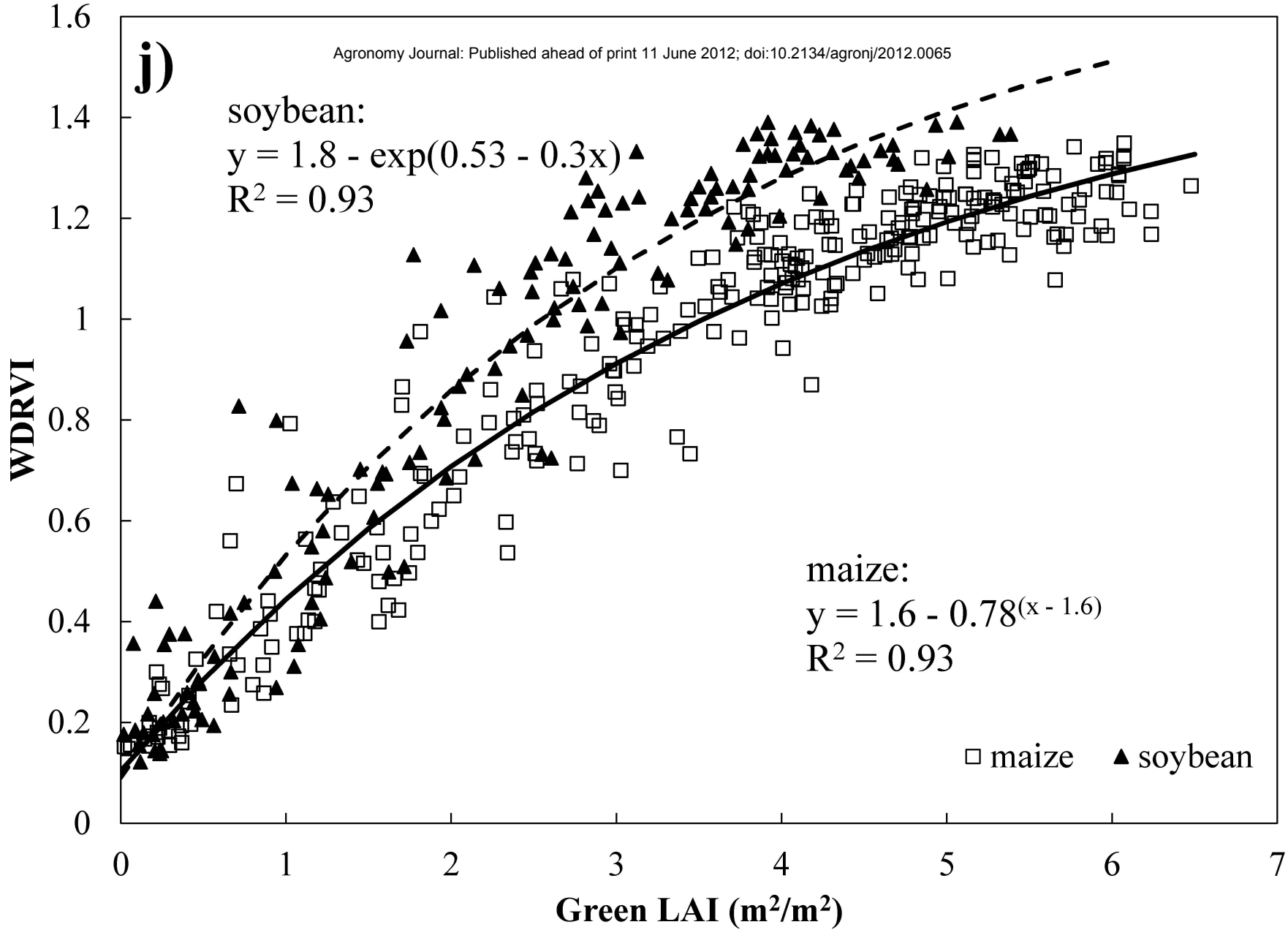
**i)**



maize:  
 $y = 1.5 + x^{1.08}$   
 $R^2 = 0.87$

soybean:  
 $y = 1.03 + x^{1.02}$   
 $R^2 = 0.82$

□ maize    ▲ soybean

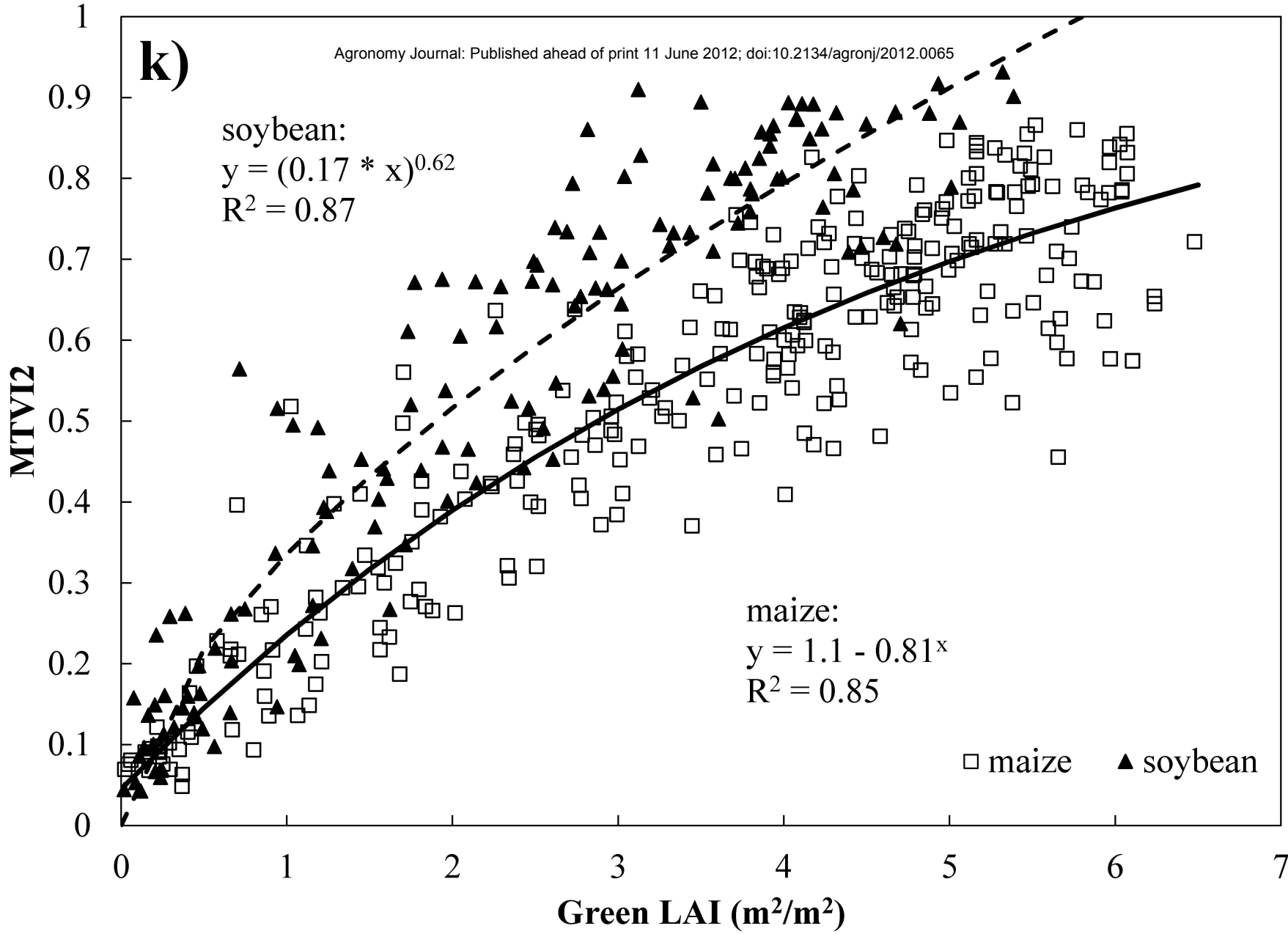


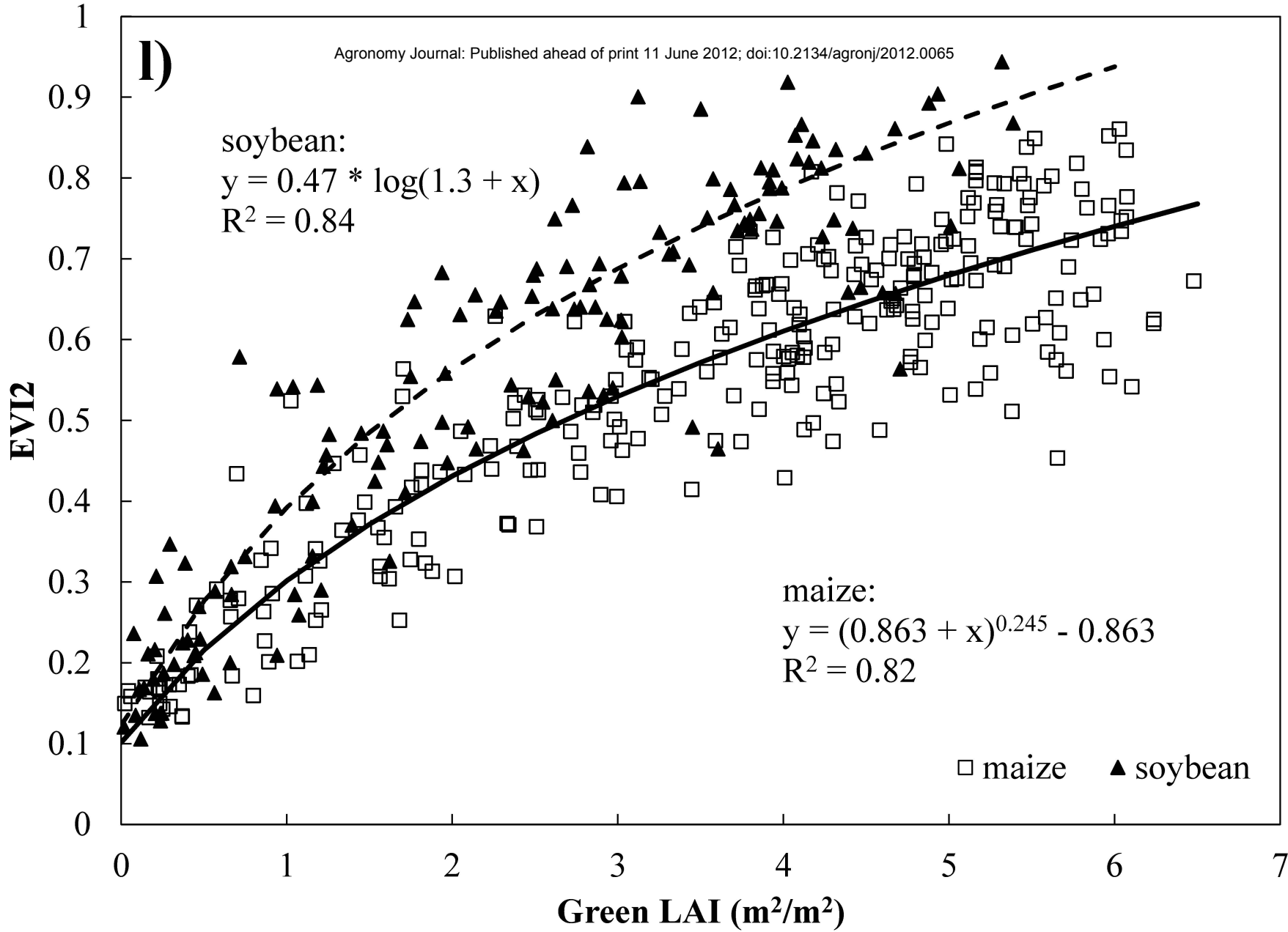
**k)**

soybean:  
 $y = (0.17 * x)^{0.62}$   
 $R^2 = 0.87$

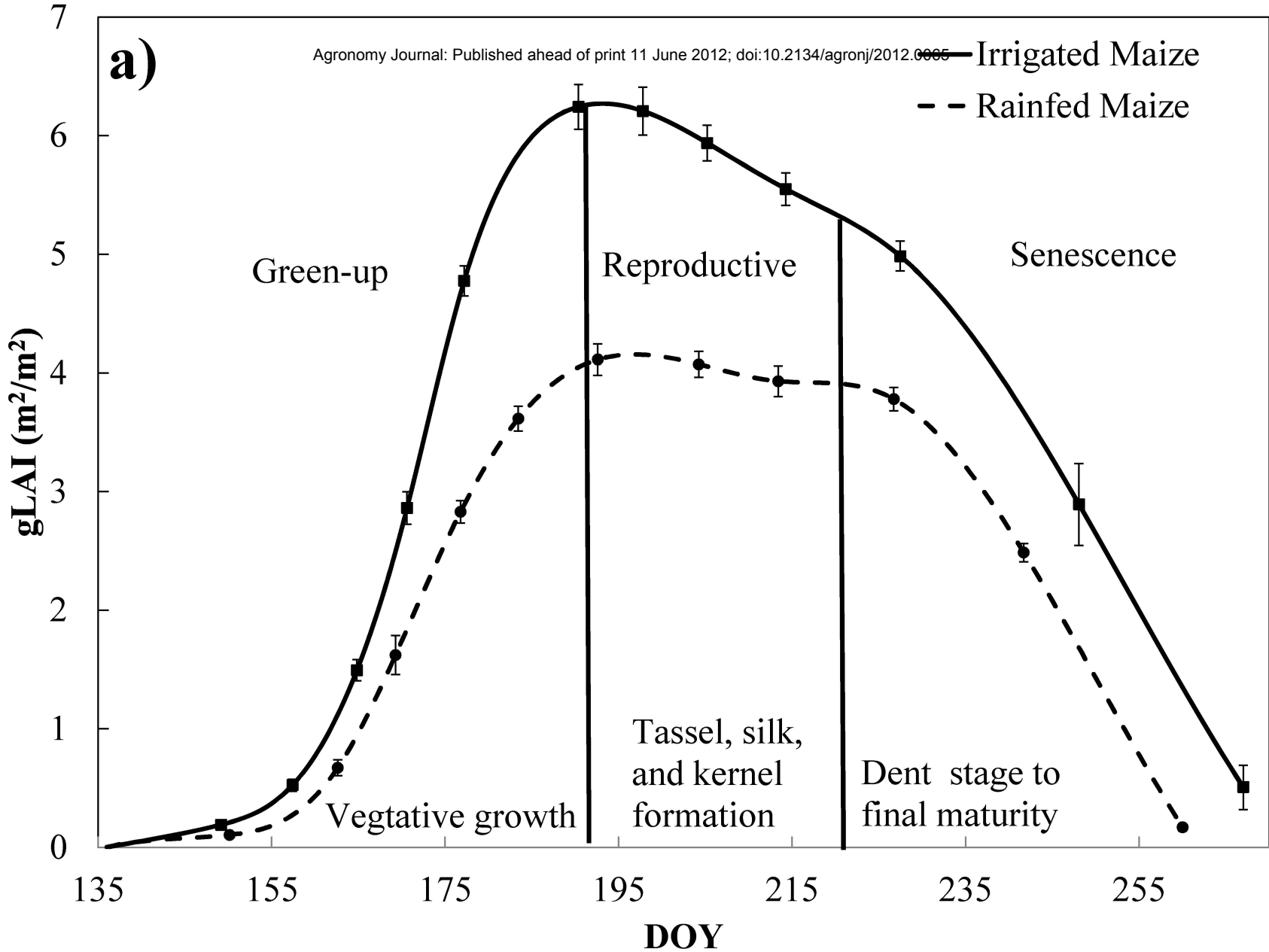
maize:  
 $y = 1.1 - 0.81x$   
 $R^2 = 0.85$

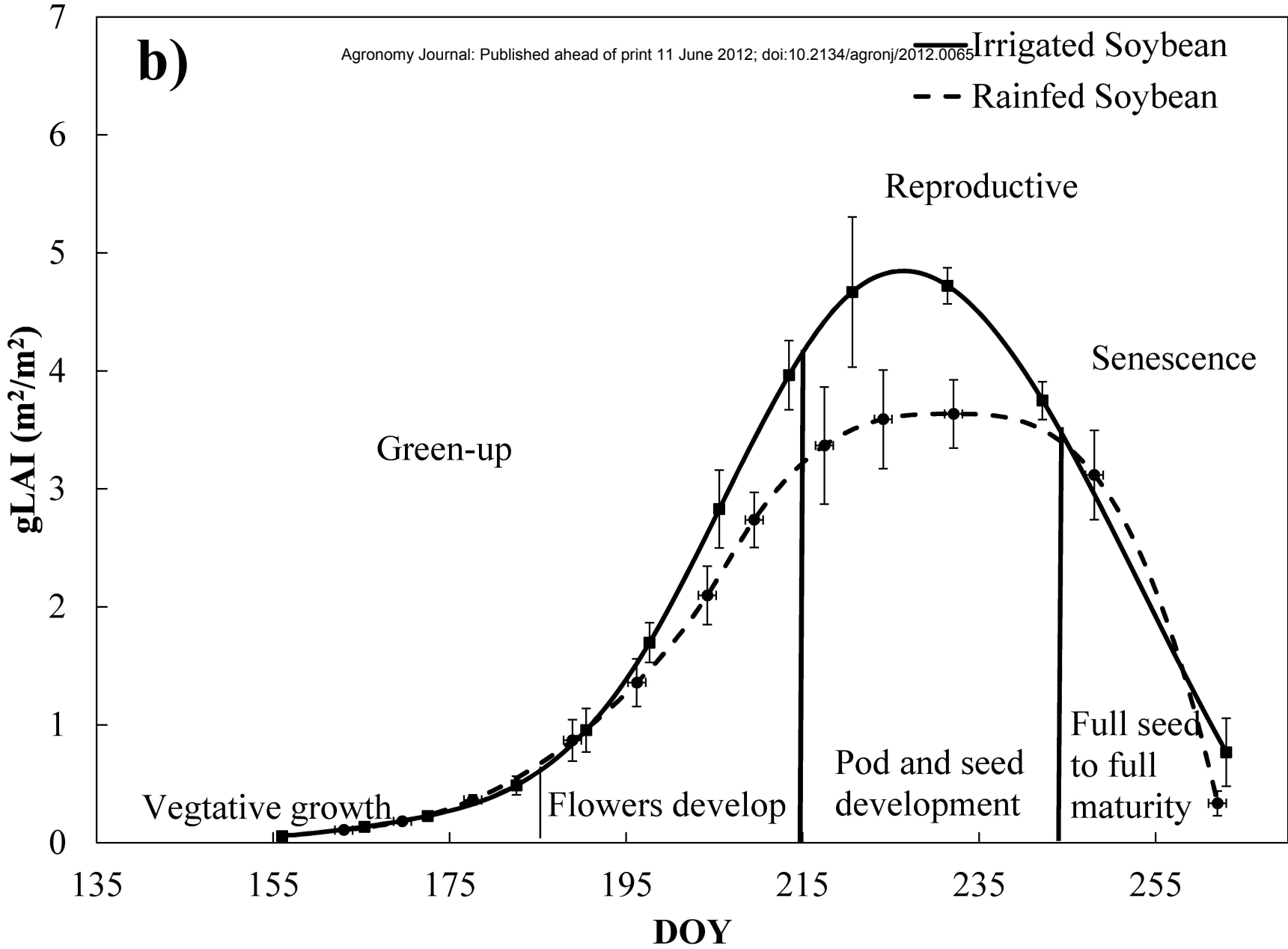
□ maize    ▲ soybean





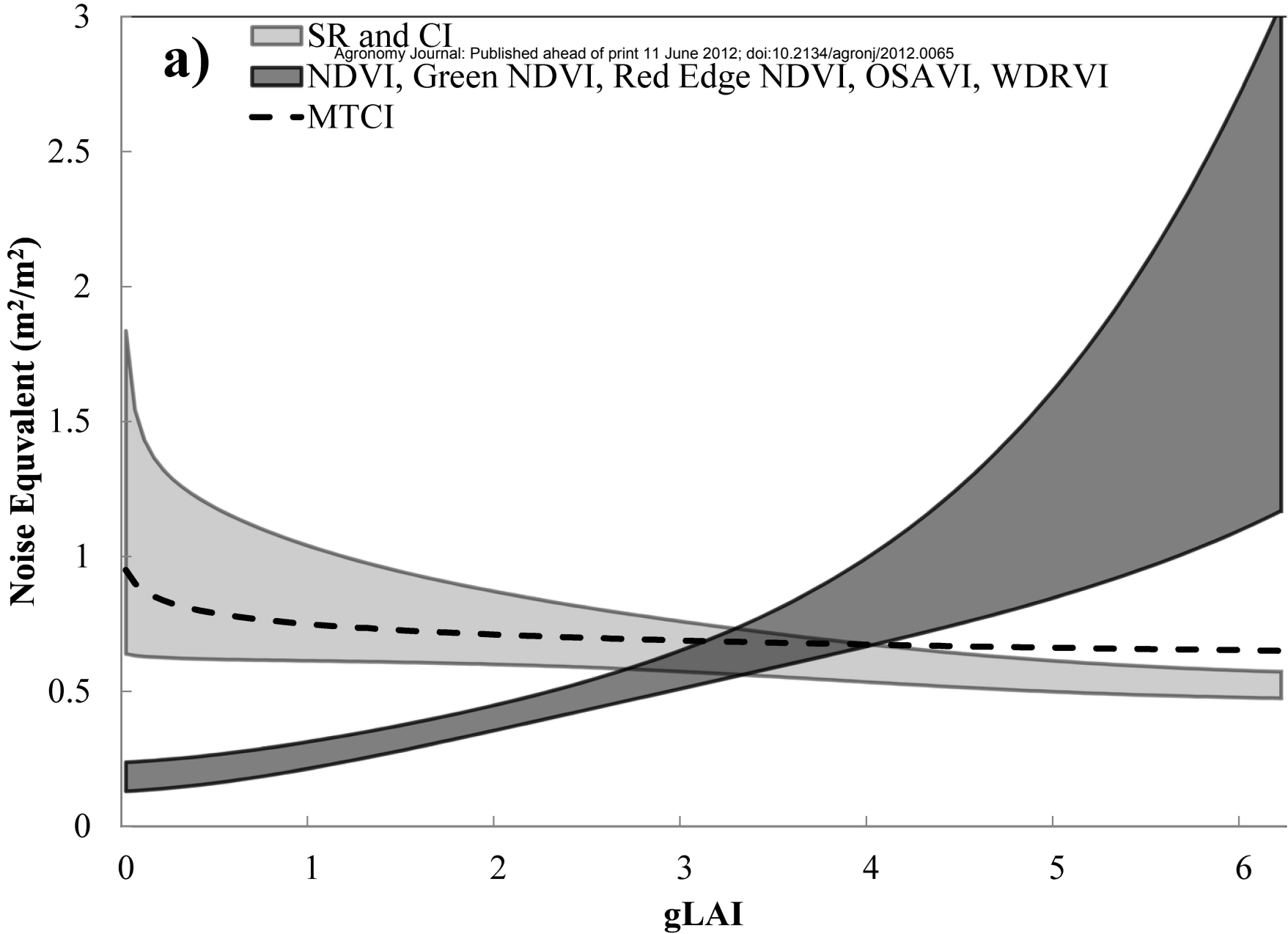
**a)**








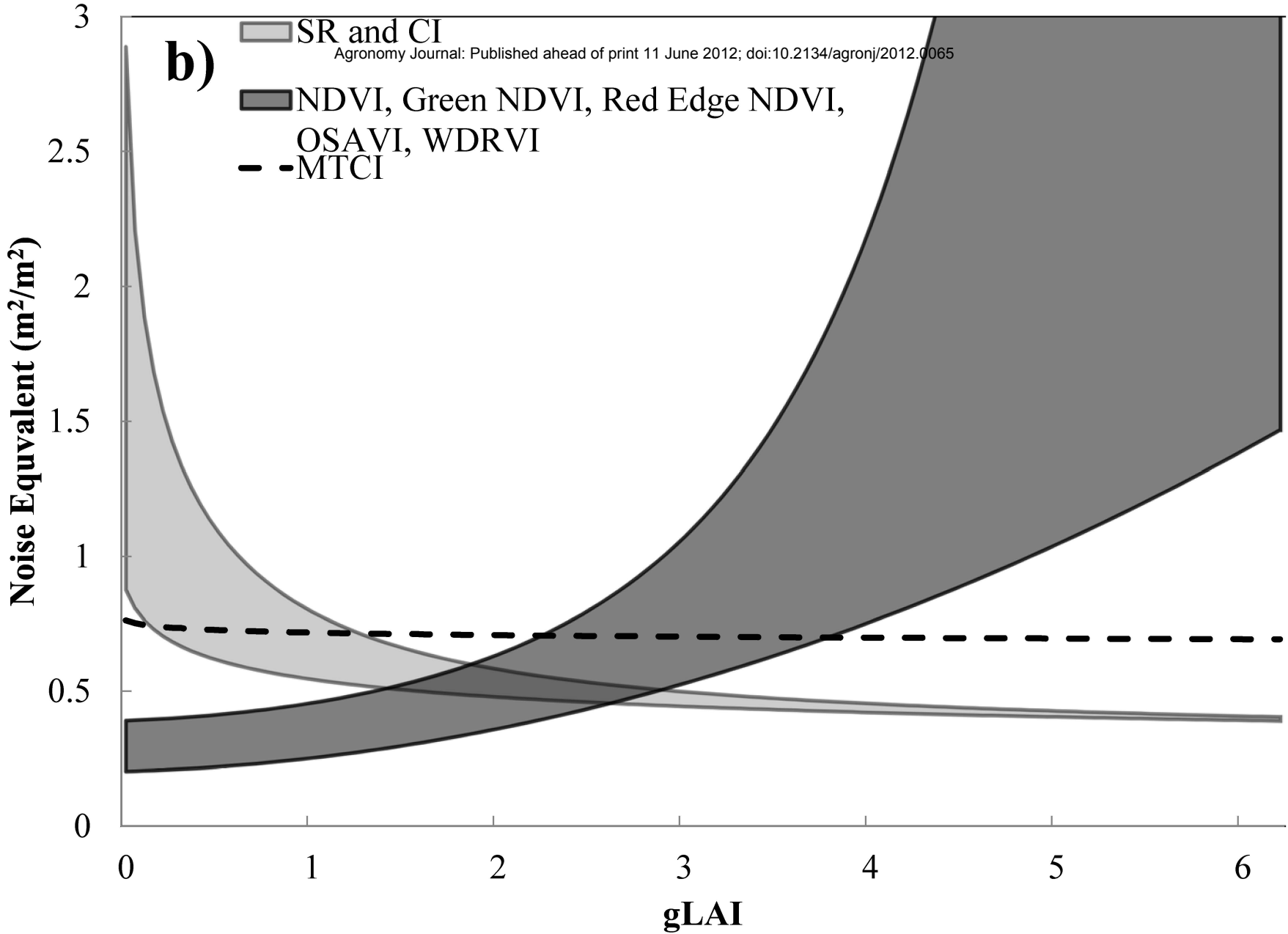
**a)**

- SR and CI
- NDVI, Green NDVI, Red Edge NDVI, OSAVI, WDRVI
- MTCI



**b)**

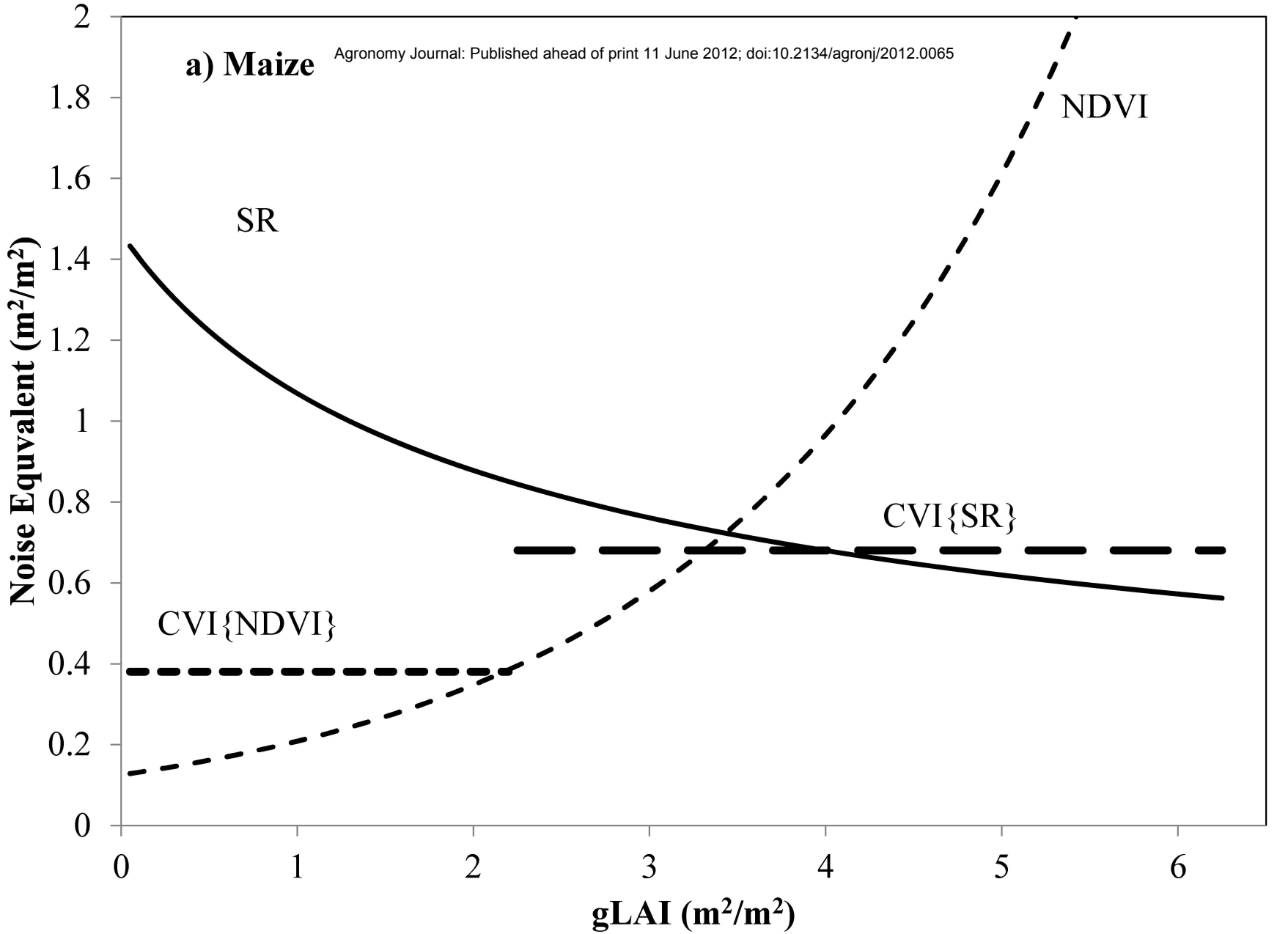
-  SR and CI
-  NDVI, Green NDVI, Red Edge NDVI, OSAVI, WDRVI
-  MTCI



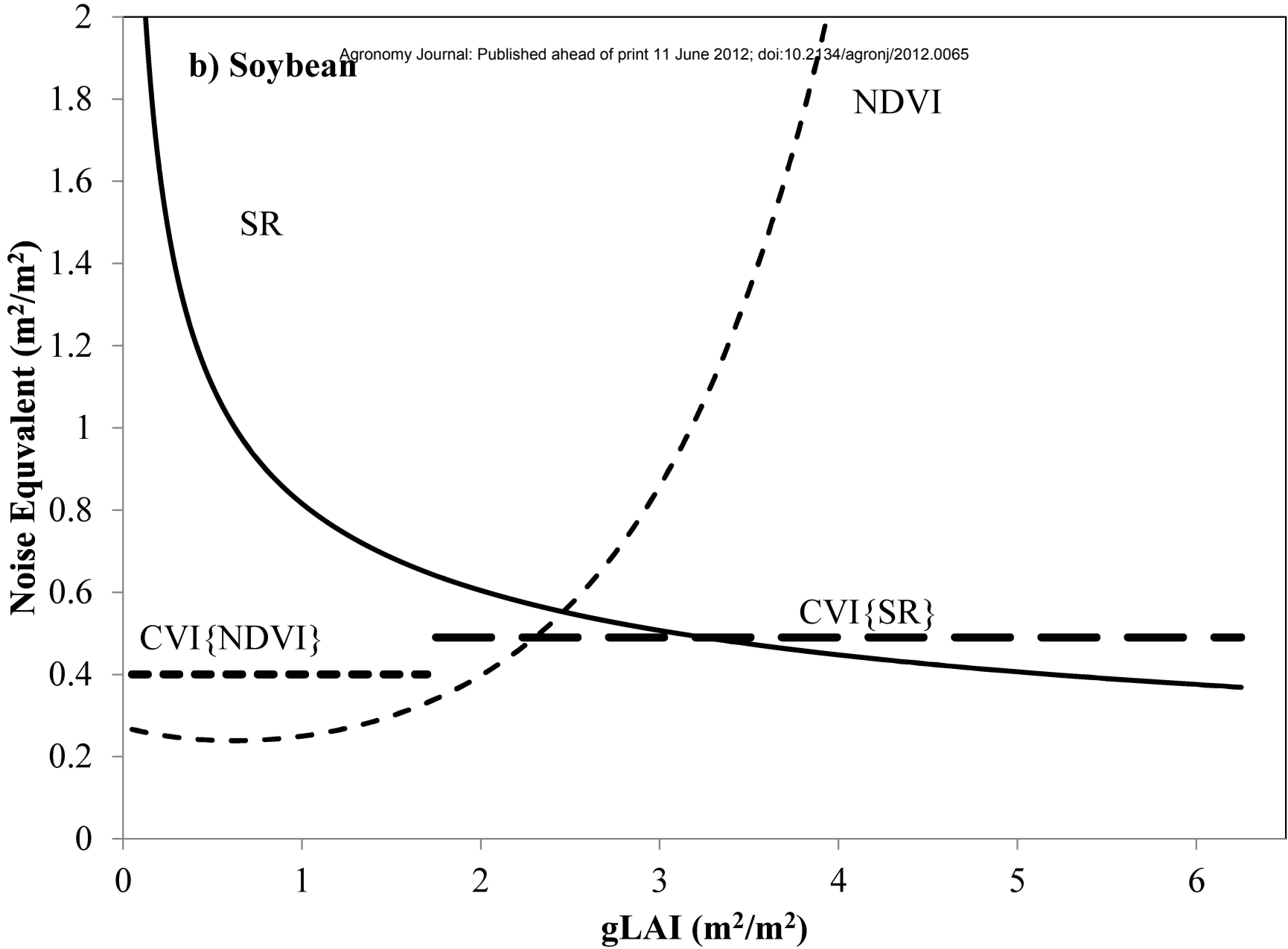


**a) Maize**

Agronomy Journal: Published ahead of print 11 June 2012; doi:10.2134/agronj/2012.0065



### b) Soybean



# Maize and Soybean

Agronomy Journal: Published ahead of print 11 June 2012; doi:10.2134/agronj/2012.0065

## Red Edge NDVI

